Fragmentation in the European Monetary Union: Is it really over? ⋆

Bertrand Candelon[a,1], Angelo Luisi[a,1], Francesco Roccazzella[a,1]

[a] *Université catholique de Louvain, Louvain Finance*

Abstract

Sovereign bond market fragmentation represents one of the major challenges European authorities have had to tackle since the outburst of the euro area debt crisis in 2010. By investigating the inter-country shock transmission through a new methodology that reconciles Factor and Global Vector Autoregressive models, we first show that fragmentation risk well preceded the sovereign debt crisis outburst. Most importantly, by analyzing the recent period, we document a rise in fragmentation risk in the euro area during the COVID pandemic. This rise, connected to the pressure on public debts and deficits due to the pandemic period, questions the European integration process and calls for early measures to avoid a new sovereign debt crisis.

Keywords: Euro Area, Sovereign bond, Fragmentation, COVID.

JEL Classification: F36, F37, G12, H63.

⋆The authors thank Christian Brownlees, and the participants at the UCLouvain CORE Brown Bag and the Insti7 internal seminars for useful comments and remarks. This research was conducted as part of the research program entitled "Financial and Extra-Financial Risk Modeling" under the aegis of the Europlace Institute of Finance, a joint initiative with Insti7. The usual disclaimer applies.

Email addresses: candelonb@gmail.com (Bertrand Candelon), angelo.luisi@uclouvain.be (Angelo Luisi), francesco.roccazzella@uclouvain.be (Francesco Roccazzella)

[1]Louvain finance, UCLouvain, Voie du Roman Pays, 34, 1348 Louvain-la-Neuve.

1. Introduction

Since the 2010-2012 European Sovereign Debt (ESD) crisis, the evolution of sovereign bonds in the euro area countries has been closely monitored. With the introduction of euro as common currency, long term yields differentials between euro area government bonds started to co-move synchronously at low rates, respecting hence the well-known property of uncovered interest rate parity in fixed exchange rate regimes. The ESD crisis completely changed this setting by leaving place to heterogeneous and unprecedented high levels of divergence among yields. Specifically, high- and low-indebted countries exhibited different patterns. The former experienced increasing yields, the latter decreasing. The fragmentation era began.

Euro Area sovereign bond yields' determinants can be summarized into three categories, global, European, and local. *Global* determinants impact all national sovereign yields evenly. Typically, they reflect the time varying risk aversion of investors in the financial markets. During distressed periods, investors demand higher compensation to invest, causing an upward shift in sovereign bond yields.

European factors affect instead the behaviour of investors in the European market. Compared to the global component, the exposure of national yields to this component can vary substantially from country to country (Georgoutsos and Migiakis, 2013). The European factors deal in fact with *intra-European* unbalances. For example, during periods of financial turmoil, investors in euro area sovereign bond markets prefer to invest in more liquid assets, the so-called "flight-to-liquidity" mechanism (Monfort and Renne, 2013). Expectations of exchange rate fluctuations traditionally belonged to this category. Exchange rate risk has been drastically reduced since the introduction of the euro. However, during the ESD crisis period, a new form of expectations of exchange rate fluctuations became sizeable, redenomination risk. It reflects the risk that, following the exit of a country from the European Monetary Union or after a hypothetical euro break up, a euro denominated asset is redenominated into a new devalued legacy currency. As shown by De Santis (2019) and Favero and Missale (2016), this risk can be particularly relevant for high-indebted countries. Moreover,

it is worth noting the heterogeneous pattern followed by high- and low-indebted countries sovereign yields' following the Greek crisis regarding debt- and deficit-to-GDP ratios in 2010 (see Figure 1).

Lastly, the local risk factors are represented by liquidity and credit risks. As shown by Favero et al. (2010) and Sgherri and Zoli (2009), liquidity risk (high transaction costs in narrow markets) is not particularly relevant for the quite mature European bond market. Credit risk is one of the most important factors in driving sovereign bond yields. It concerns the ability of a country to repay its public debt at a finite horizon. Before the Great Financial Crisis, this component accounted for almost the whole observed dynamics in sovereign yields (Favero and Missale, 2012). Fundamental determinants of the default related component of yields are macroeconomic and financial fundamentals such as Gross Domestic Product (GDP) growth, debt- and deficit-to-GDP levels.

Several studies have tried to disentangle these three components aiming at better evaluating and forecasting the fragmentation risk on the sovereign bond markets. Sgherri and Zoli (2009) consider a dynamic state-space model to extract the common factors across European sovereign bonds. They show the predominance of common factors before the ESD crisis and the importance of specific factors after. Favero and Missale (2012) prefer to opt for a Vector Autoregression (VAR) representation to model it. They stress the importance of market sentiment. Global and European appetite for risk is therefore not constant over time, signaling the presence of contagion driven by shifts in the market sentiment. More recently, Favero (2013) considers a Global VAR ($GVAR$) representation. $GVAR$ builds on local VAR models, augmented by the so-called *star* variable, i.e., weakly exogenous weighted averages of foreign variables, resulting in local $VARX^*$ models (Harbo et al., 1998; Pesaran et al., 2004). The key point of these models is the W matrix of weights that relates the local models to foreign counterparts. Favero (2013) considers interconnection in terms of fiscal fundamentals, the more similar two countries are in terms of debt- and deficit-to-GDP ratios, the tighter is the interconnection between their sovereign yields. Indeed, Favero (2013) shows that sovereign

bond markets of high-indebted countries started to be more and more interconnected from 2005 onward. However, Candelon and Luisi (2020) prove that, in the case of sovereign bond markets in the euro area, weights are statistically misspecified if constrained to be non negative. The nonnegativity constraint on weights forbids to consider simultaneously "contagion" (positive transmission among distressed markets) and "flight-to-quality" (negative transmission from distressed to safe markets) *phenomena*. Thus, they show it is optimal to consider two different W matrices, that associated with a negative coefficient (W^-) and that associated with a positive coefficient (W^+) in the local $VARX^*$ models. Using this approach, they show that fragmentation risk signs were important even prior the ESD crisis among European countries.

This paper reconciles the factor augmented VAR ($FAVAR$) and the $GVAR$ literature, by employing (static) principal components (PC) as a way to retrieve information from cross sectional dependence. Specifically, as in Elhorst et al. (2020), we confirm that in presence of high cross sectional correlation, the first PC captures the common factor underlying sovereign bond markets. This factor can be interpreted as the *global* factor. The second PC provides guidance for the presence of *intra-European* interconnection expressed as the idiosyncratic contribution to the residual cross sectional correlation. We therefore follow the intuition of Bernanke et al. (2005), and retrieve the part of the second PC that is unspanned by the specific local market under analysis (i.e. *foreign* information). We express this component as the weighted average of foreign counterparts (in the $GVAR$ fashion), but leaving the sign of the weights unconstrained. The analysis of the resulting transmission matrix W provides evidence of the presence of "flight-to-quality" and/or "contagion" effects in the euro area.

This methodology is implemented for long term yield spreads between the 10 year euro area government bonds and the German safe benchmark over three remarkable periods: The pre-ESD crisis, the post-ESD crisis as well as the recent COVID period. It is noticeable that signs of "contagion" and "flight-to-quality" effects were already present in the pre-ESD crisis period, pointing out at a latent fragmentation risk between Peripheral European countries

(Portugal, Italy, Ireland, Greece and Spain) and the Core ones (Austria, Belgium, Finland, France, and The Netherlands). Such a finding contradicts existing literature regarding financial integration in the euro area before the ESD crisis period (see, for example, Baele et al., 2004) but is in line with the recent results of Candelon and Luisi (2020). Soon after the ESD crisis, the different programs of public bonds purchases enhanced by the European Central Bank have reduced this risk, leading all European spreads to shrink back slowly but steadily to the pre-ESD crisis period (even if we still document a tighter interconnection among Peripheral countries). The COVID pandemic has pushed again the fragmentation risk at the forefront of the results. Despite the implementation of the European recovery program, "contagion" and "flight-to-quality" effects became evident once again, stressing the revival of fragmentation risk.

The paper is sketched as follows: after a preliminary data analysis in Section 2, the methodology is presented in Section 3. The empirical analysis on the fragmentation risk is performed in Section 4. while Section 5 concludes.

2. Preliminary Data analysis

We start our analysis by examining the dynamics of the long term yield differentials between euro area government bonds. The 10 years weekly yields are extracted from Refinitiv Eikon data set and are covering 11 countries (Austria, Belgium, Finland, France, Germany, Greece, Ireland, Italy, the Netherlands, Portugal and Spain) over the period June 2006 - March 2021 and shown in Figure 1.

What emerges from a first visual inspection is that long term yields differentials between euro area government bonds and the German *safe* benchmark co-move following an unstable pattern over time.

In the following sections, we give a closer look at this dynamics, distinguishing across the pre- (June 2^{nd}, 2006 - March 26^{th}, 2010), during- (April 2^{nd}, 2010 - July 27^{th}, 2012), and post- (August 1^{st}, 2012 -), ESD crisis periods. On the one hand, April 2010 is the indicative

watershed that certifies the beginning of the European sovereign debt crisis. In particular, after the publication of the Greek quarterly national accounts data which signaled a persistent recession for the Hellenic economy starting in 2007, credit rating agencies then downgraded Greek bonds to the investment grade status in late April 2010. On the other hand, on the July 26^{th}, 2012 the President of the European Central Bank Mario Draghi pronounced the famous "Whatever it takes" speech, announcing the Outright Monetary Transactions ($OMTs$) to neutralize the risk of a euro break up. [2]

Long term sovereign bond spreads over the German *Bund* in Europe

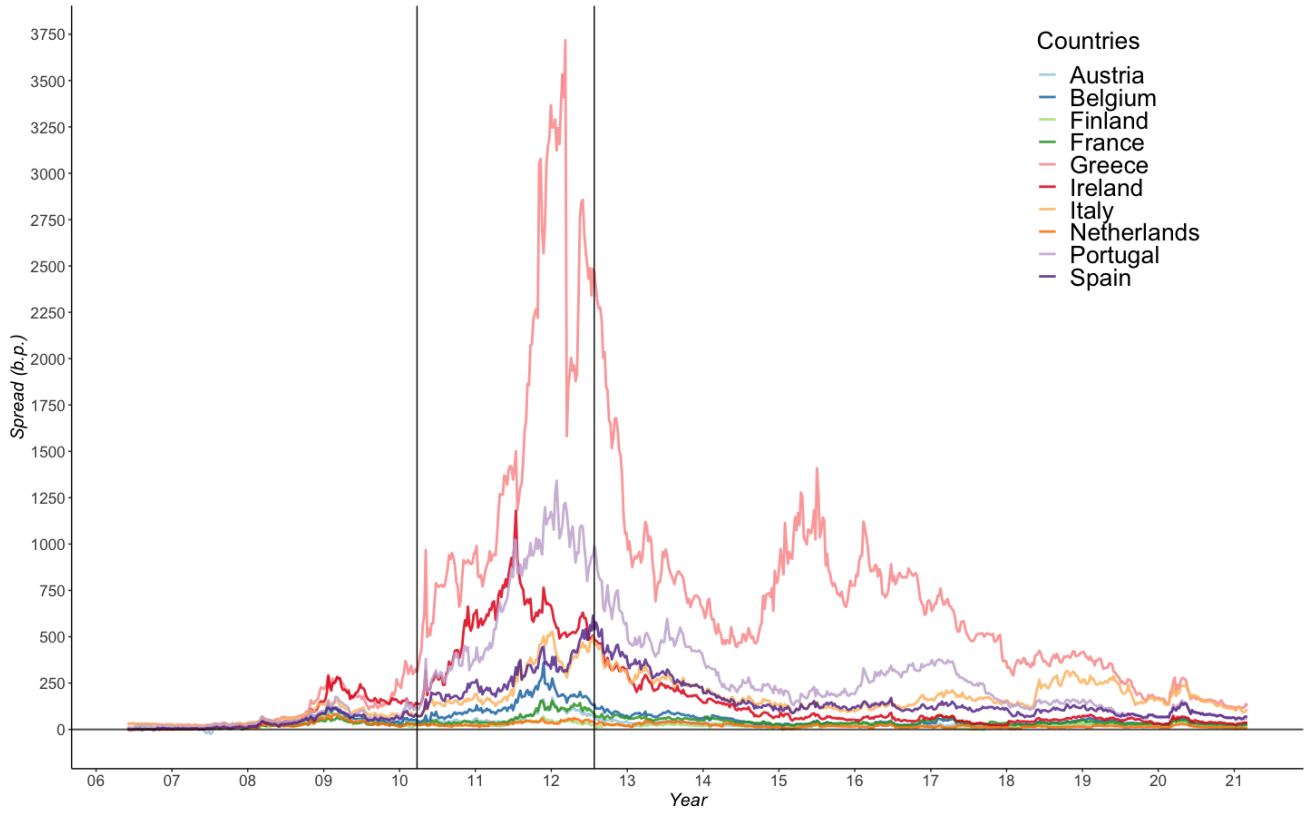

Figure 1: The figure reports the evolution of the government bond yield spread of 10 countries (Austria, Belgium, Finland, France, Greece, Ireland, Italy, the Netherlands, Portugal and Spain) vis á vis of Germany over the period 2006 June - 2021 March. The EDS crisis beginning and end dates are indicated with vertical bars.

[2]The verbatim of the speech by Mario Draghi is available at `https://www.ecb.europa.eu/press/key/date/2012/html/sp120726.en.html`

2.1. Pre-ESD crisis period

The dynamics of the spreads during the pre-ESD crisis period can be further decomposed into a convergence period and the subprime loans crisis period. In fact, despite market participants have never regarded the long term bonds issued by other euro area Member States as perfect substitutes of the German *Bund* (Favero and Missale, 2012), interest rate differentials co-moved synchronously at a very low level until the burst of the subprime loans crisis. During 2008 and 2009, $10Y$ sovereign debt spreads became considerable. At this point the joint dynamics of euro area spreads began to fracture: a separate co-movement between high-debt and low-debt countries emerges. (Favero, 2013).

2.2. The ESD crisis period

The ESD crisis brought even greater magnitude in the $10Y$ differentials than those of the $2008 - 2009$ period and a marked heterogeneity in their co-movement. The idea that long term government debt spreads follow a common dynamics in the euro area fades away: the Core (Germany, France, Belgium, Netherlands, and Finland) and Periphery (Greece, Ireland, , Italy, Portugal and Spain) binary classification becomes predominant both in the political and academic debate when analysing the economic and financial turmoil in $2010 - 2012$ (House et al., 2020; Corsetti et al., 2014).

During the fall of 2011, the $10Y$ differentials relative to the German *Bund* reached record heights: Italian $10Y$ sovereign yield spreads rising in a few weeks from 270 basis points in August to over 500 basis points in November. We can draw a similar picture for Ireland, Portugal and Spain. However, it seemed that such outcomes were only partially connected to underlying fiscal fundamentals (De Grauwe and Ji, 2012), as they also reflected self-fulfilling prophecies and the existence of multiple *equilibria* (Corsetti and Dedola, 2016; Cole and Kehoe, 2000). In early 2012, the risk of euro area break up became so real that the Euro redenomination risk, i.e., is the risk that a euro asset is redenominated into a devalued legacy currency, significantly impacted sovereign yield spreads, with Italian and Spanish bonds being most negatively affected (De Santis, 2019).

Following Mario Draghi's, "whatever it takes" speech, the ECB announced a new set of unconventional measures, the Outright Monetary Transactions ($OMTs$). This programme explicitly aimed at relieving the financial fragmentation in the euro area and at neutralizing redenomination risk. As a fact, by September 2012, Irish, Italian, Portuguese and Spanish differentials relative to the German $10Y$ yield had already decreased by an average of 200 basis points. Through the public purchasing programs (Securities Markets Programme), the very long term refinancing operations ($VLTROs$), and the announcement of the $OMTs$, the ECB mitigated the fears in sovereign bond markets, reinforcing a slow but progressive return of spreads towards normal levels.

2.3. The post-ESD crisis period

The third period under analysis starts in August 2012, spanning the slow but steady return of spreads towards pre-crisis levels till March 2020, when the explosion of the COVID pandemic and the enhancement of the first travelling restrictions and lockdown measures across Europe started to be implemented.

In late 2012, ECB's actions addressed the difficulties in the transmission of the monetary policy measures, the onset of a credit crunch, and the risk of deflation.[3]

As a result of these measures, the consolidated balance sheet of the Eurosystem has more than doubled between 2010 and 2020, starting from $2,002,210$ EUR millions in 2010

[3]More precisely, in July 2013, the ECB began using forward guidance with the goal of strengthening the monetary policy transmission mechanism from short to long term interest rate. In June 2014, the ECB further cut the main marginal lending facility rate to 0.4%, the refinancing operation rate to 0.15% and lowered the deposit facility rate to -0.10%. A series of the targeted longer-term refinancing operations ($TLTROs$) (June 2014, March 2016 and March 2019) have also been used to stimulate bank lending to the real economy. Starting in mid-2014, the ECB also launched the Asset Purchase Programme (APP), conducting net purchases of corporate sector ($CSPP$), public sector ($PSPP$), asset-backed securities ($ABSPP$) and covered bond ($CBPP3$).

and reaching $4,671,425$ EUR millions in 2019.[4] Consequently, given the massive liquidity injections operated by the ECB during the 2012 - 2020 period, the progressive decline of the $10Y$ government bond differentials relative to the German *Bund* should not come as a surprise.

2.4. The COVID pandemic period

At the outbreak of the COVID pandemic in Europe in March 2020, euro area $10Y$ sovereign spreads suddenly increase. In this period, the European Commission, the European Parliament and EU countries have been seeking for an agreement to help repairing the economic and social damages caused by the Coronavirus pandemic and boost the recovery at the European level. In December 2020, the agreement for a 1.8 trillion EUR recovery plan was reached together with the return of generalized common and declining co-movement in the dynamics of $10Y$ government debt spreads. The novelty of this recovery plan is that it will be issued by the European Union as a whole and the associated debt will not be recorded in the countries national accounts. It should result in reducing the risk premium and foster the link among European countries.

3. Methodology

3.1. GVAR Models as approximation of Factor Models

The use of the Factor Model as a theoretical justification of $GVAR$ as a framework to model international interconnections comes from Dees et al. (2007). Assume that there are N countries in the global economy, and that our aim is to model the k_i with $i = 1, \ldots, N$ local macro-economic and/or financial variables collected in the vector x_{it} over time $t = 1, \ldots, T$.

---

[4]The Eurosystem consolidated balance sheet is published together with the Annual Accounts, and is included in the Annual Report of the ECB. The data is available at `https://www.ecb.europa.eu/pub/annual/balance/html/index.en.html`

Given the general nature of interconnections, a good starting point for the analysis is the factor model:

$$x_{it} = \delta_{i0} + \delta_{i1}t + \Gamma_{id}d_t + \Gamma_{if}f_t + \epsilon_{it} \tag{1}$$

for $i = 1, \ldots, N$, and $t = 1, \ldots, T$. d_t represents the vector of the m_d global observed factors, f_t the m_f unobserved global factors. $\Gamma_i = (\Gamma_{id}, \Gamma_{if})$ is the $k_i \times m$ matrix collecting the factor loadings with $m = m_d + m_f$. ϵ_{it} is the vector of country specific effects.

To allow for cointegration and unit root properties of x_{it}, Dees et al. (2007) further assume that:

$$\Delta h_t = \Lambda(L)\eta_t, \quad \eta_t \overset{i.i.d.}{\sim} (0, I_m) \tag{2}$$

$$\Delta \epsilon_{it} = \Psi_i(L)\nu_{it}, \quad \nu_{it} \overset{i.i.d.}{\sim} (0, I_{k_i}) \tag{3}$$

with L being the Lag operator. Dees et al. (2007) prove that in such a setting factors can be approximated by cross sectional averages:

$$f_t \xrightarrow{q.m.} (\Gamma_f^{*\prime}\Gamma_f^*)^{-1}\Gamma_f^*(x_t^* - \delta_0^* - \delta_1^* t - \Gamma_d^* d_t - \epsilon^*). \tag{4}$$

The *star* variables being cross sectional averages of the initial variables in (1). The $GVAR$ framework, instead of considering the same factor for all countries under analysis, employs country specific ones built as weighted averages of foreign counterparts, where the weights capture the tightness of the interconnection between country i and country j as follows:

$$x_{it}^* = \sum_{j=0}^{N} w_{ij} x_{jt}, \quad w_{ii} = 0, \quad \sum_{j=0}^{N} w_{ij} = 1 \tag{5}$$

resulting in the local $VARX^*$ model counterpart of (1):

$$\Phi_i(L, p_i)x_{it} = a_{i0} + a_{i1}t + \Upsilon_i(L, q_i)d_t + \Lambda_i(L, q_i)x_{it}^* + \nu_{it}, \tag{6}$$

where p_i and q_i are the maximum lag considered for the local and foreign variables, respectively. The different coefficients are treated as unrestricted for estimation purposes.

For a correct interpretation of the country specific weights employed, it is fundamental to disentangle the common components from the cross-sectional interactions when the different series are strongly co-moving along a common trend (Elhorst et al., 2020). This can be achieved in a two step approach as in Bailey et al. (2016a), *defactorizing* the observations and then modeling the residual cross sectional dependence. Vega and Elhorst (2016) argue against the two step approach in favour of a simultaneous approach. As observable measure of the unobserved factors, Principal Component (PC) analysis can be effectively employed (see, for example, Stock and Watson, 2016). Moreover, Bernanke et al. (2005) show that it is possible to disentangle the part of the information spanned by the PCs that is external to the specific local variables considered. Finally, the factors summarizing the *external* information can be included in a VAR specification as (weakly) exogenous variables following Balabanova and Brüggemann (2017).

Once local parameters in (6) are estimated, we can simultaneously solve the model to obtain the *Global VAR* representation of the world. We now summarize the procedure as in Pesaran et al. (2004).

Define the $(k_i + k_i^*) \times 1$ vector:

$$z_{i,t} = \begin{pmatrix} x_{i,t} \\ x^*_{i,t} \end{pmatrix} \tag{7}$$

and rewrite (6) as:

$$A_i z_{i,t} = B_i z_{i,t-1} + \epsilon_{it} \tag{8}$$

with $A_i = (I_{k_i},\ -\Lambda_{i0})$ and $B_i = (\Phi_i,\ \Lambda_{i1})$. For ease of explanation, we here abstract, without loss of generality, from including the deterministic component, the time trend, and additional lags.

If we collect all the local variables in $x_t = (x'_{0t}, x'_{1t}, \ldots, x'_{Nt})'$ for $i = 1, \ldots, N$ with

$k = \sum_1^N k_i$, we can rewrite:

$$z_{i,t} = W_i x_t. \tag{9}$$

By substituting (9) into (8), we obtain:

$$A_i W_i x_t = B_i W_i x_{t-1} + \epsilon_{it}, \tag{10}$$

Stacking all the equations together:

$$G x_t = H x_{t-1} + \epsilon_t, \tag{11}$$

As in Candelon and Luisi (2020), by defining the interaction matrix $\tilde{W}$ as:

$$x_t^* = \tilde{W} x_t. \tag{12}$$

We can express the matrices G and H as:

$$G = [I_k - \tilde{\Lambda}_0 \tilde{W}] \tag{13}$$

$$H = [\tilde{\Phi} + \tilde{\Lambda}_1 \tilde{W}] \tag{14}$$

Lastly, we can retrieve the $GVAR$ solution as:

$$x_t = G^{-1} H x_{t-1} + G^{-1} \epsilon_t. \tag{15}$$

Therefore, the $GVAR$ solution is the reduced form VAR representation of the world. This representation is particularly useful for forecasting, scenario analysis and Generalized Impulse Response function.

3.2. Taking the model to the data: Sovereign spreads in the euro area

GVAR Models have been employed in the analysis of the interactions among European sovereign bonds spreads as a tool to unveil the tightness of financial interconnectedness and to identify the transmission channels of asymmetric shocks. Favero (2013) showed that the cross correlation among sovereign bond spreads follows an unstable pattern over time, implying that a correct proximity measure should take into account the shifts described in the preliminary data analysis in Section 2. Moreover, Favero and Missale (2012) showed how a shift in market sentiment following the emergence of a country financial distress can propagate to relatively safer countries. For example, they estimate that a shock in August 2011 could trigger a contagion on the Italian sovereign yield of the size of 200 basis points.

Following Favero and Missale (2012), the local *GVAR* specification in the case of sovereign bond spreads over the German *Bunds* $(Y_t^i - Y_t^{DE})$ can be expressed as follows:

$$(Y_t^i - Y_t^{DE}) = \beta_{i0} + \beta_{i1}(Y_{t-1}^i - Y_{t-1}^{DE}) + \beta_{i2}(Y_t^i - Y_t^{DE})^* + \beta_{i3}(Y_{t-1}^i - Y_{t-1}^{DE})^* + u_t^i \qquad (16)$$

where $i = 1, \ldots, N$ is the specific country under analysis, β_{i0} the deterministic component, β_{i1} the coefficient associated with the country specific lagged variable, and β_{i2} and β_{i3} the coefficients associated with the (contemporaneous and lagged) *Global Spreads*, $(Y_t^i - Y_t^{DE})^*$. *Global Spreads* are computed for each country as the weighted average of foreign counterparts' spreads over the German *Bund*, $\sum_{i \neq j} w_{ij}(Y_t^j - Y_t^{DE})$ for each $i \neq j$.

As recommended by Elhorst et al. (2020), we first perform the *CD*-test (Pesaran, 2021) on the cross section of spreads to prove their strong co-movement along a global trend (see Section 4). Based on this result, we augment the *GVAR* specification in (17) as follows:

$$(Y_t^i - Y_t^{DE}) = \beta_{i0} + \beta_{i1}(Y_{t-1}^i - Y_{t-1}^{DE}) + \beta_{i2}(Y_t^i - Y_t^{DE})^* + \beta_{i3}(Y_{t-1}^i - Y_{t-1}^{DE})^* + \beta_{i4}\hat{F}_{1,t} + u_t^i \quad (17)$$

where $\hat{F}_{1,t}$ is the first Principal Component (PC) extracted from the cross-section of yields.[5]

The common factor $\hat{F}_{1,t}$ can therefore be interpreted as a long run stable attractor proxying the global interdependence among European countries' sovereign bonds. By augmenting our specification in this way, we make sure that the *star* variables in (17) and the associated coefficients deal with *intra-European* interconnection defined in a $GVAR$ fashion.

The choice of the weights employed to build the *Global Spreads* is crucial. As outlined in Subsection 3.1, the $GVAR$ specification demands the weights to summarize the *external* information through a weighted average of foreign counterparts. Existing literature has shown that misspecifying the channel of interconnection results in incorrect inferences (see, for example, Gross, 2019). Candelon and Luisi (2020) show that in the case of euro area sovereign bond spreads, an empirically valid channel of interaction should take into account the asymmetric transmission of shocks among countries that exhibit positive (negative) interconnections.

Therefore, it is natural to start the interconnection analysis from the second factor of the cross section of sovereign spreads for several reasons. First, the second Principal Component $\hat{F}_{2,t}$ summarizes the cross sectional information that is linearly independent to the first factor $\hat{F}_{1,t}$, therefore its inclusion in (17) would not be problematic from an econometric perspective. Second, by construction $\hat{F}_{2,t}$ is designed to explain most of the cross sectional variance left unexplained by $\hat{F}_{1,t}$, capturing therefore the interconnection among spreads as we aim to. Third, the loadings of the factors are not constrained to be nonnegative, providing guidance for not only the size, but also the sign of the weight of each local yield contribution to the cross sectional variance explained. Four, it allows us to follow the intuition in Bernanke et al. (2005) and extract from the Principal Component the *foreign* information, as requested by

[5]Observable common variables are often also employed in the literature for this purpose (for example, Favero, 2013, augments the specification with the long term corporate *Baa-Aaa* spread to account for global risk aversion).

the *GVAR* framework, where the *Global* variable is a weighted average of foreign counterparts. Finally, the inclusion of the factors summarizing external information as (weakly) exogenous variable can be included in a typical $VARX^*$ fashion (see, for example, Balabanova and Brüggemann, 2017).

For all these reasons, we consider:

$$\hat{F}_{2,it} = \sum_{i \neq j} w_{ij}(Y_t^j - Y_{t-1}^{DE}) + v_{it} \tag{18}$$

for every $i = 1, \ldots, N$ with $\sum_{i \neq j} |w_{ij}| = 1$. $\hat{F}_{2,it}$ is the part of the second Principal Component that is unspanned by the local economy i taken into account (see Appendix A). Usually in the *GVAR* literature, the weights are constraint to be nonnegative. However, the normalization we propose allows keeping the original properties of the size of the weights (Pesaran et al., 2004), while considering also that sovereign bond spreads' interconnections can be positive and negative. Relaxing the nonnegativity assumption becomes particularly relevant when mechanisms as "contagion" (see Metiu, 2012; Candelon and Tokpavi, 2016) or "flight-to-quality" (Monfort and Renne, 2013) are present. Specifically, during distressed periods, investors prefer safer and more liquid assets. This would result in an outflow of money from the Peripheral to the Core countries, causing rising yields for the high indebted euro area members ("contagion") while financial sounder economies could benefit from lower rates ("flight-to-quality"). In our framework, this possibility is not ruled out thanks to the unrestricted sign of the weights.

Once the weights are retrieved by estimating (18) with OLS, we can build the foreign weighted averages as of (5) and estimate the local $VARX^*$ systems as specified in (17).

Armed with the local coefficients, we can proceed to solving the model in order to retrieve the *GVAR* representation in (15).

4. Results

4.1. Preliminary results

Following Favero and Missale (2012), and given the data analysis outlined in Section 2, we consider two separate periods: pre-ESD crisis (June 2006 to March 2010) and post-ESD crisis (from August 2012). Moreover, the COVID period is separately analyzed to further study the last part of the sample, where sovereign spreads seem to be back to the pre-ESD crisis co-movements, despite the COVID crisis.

The sample split offers several advantages. First of all, by considering homogeneous periods in terms of cross correlation of the spreads, we can assess the changes in inter-connectedness in those different phases (Forbes and Rigobon, 2002), while accounting for the observed shifts in market sentiment (Favero and Missale, 2012). Furthermore, using a narrative approach, the effect of the unconventional monetary policies in fostering financial integration can be assessed (Favero and Missale, 2016).

The first result reported in Table 1 regards the *CD*-test to assess the cross sectional dependence of the sovereign spreads under analysis. The *CD*-test (Pesaran, 2021) is defined as:

$$CD = \sqrt{\frac{2T}{N(N-1)}} \sum_{i=1}^{N-1} \sum_{j=i+1}^{N} \hat{\rho}_{ij} \tag{19}$$

with $\hat{\rho}_{ij}$ being the sample correlation coefficient between local variables of county i and country j. In Bailey et al. (2016a), we can find the order property of the average correlation coefficient:

$$\bar{\rho}_N = \frac{2}{N(N-1)} \sum_{i=1}^{N-1} \sum_{j=i+1}^{N} \rho_{ij} = O(N^{2\alpha-2}), \tag{20}$$

where $\alpha \in [0, 1]$. As recommended in Elhorst et al. (2020), we first control that the null of weak cross sectional dependence ($\alpha < 0.5$) cannot be rejected in our sub-samples through the *CD*-test ($\hat{\bar{\rho}}$ and CD-statistic's columns in Table 1). Given the results, weak cross sectional dependence cannot be rejected given the high value of $\hat{\bar{\rho}}$.

Secondly, we assess the degree of cross sectional correlation through the two step procedure

as in Bailey et al. (2016a).[6] In Table 1 we show that the cross sectional correlation in the subsamples under analysis is really strong. Specifically, the estimated α is larger than 3/4, clearly pointing at the presence of common components at the basis of the behaviour of sovereign spreads. To correctly capture the interconnections among spreads, it is therefore important to *defactorize* the data. Following Vega and Elhorst (2016), we opt for a simultaneous approach as specified in (17).

To further document that *defactorizing* the data is important (and that no interconnection among units is considered at this stage), we show in Table 2 the loadings of the first Principal Component. As expected in such a case, the loadings are evenly distributed among the different sovereign spreads under analysis. Hence, it supports the evidence of a persistent interdependence trend among European sovereign yield spreads.

Table 1: Cross sectional dependence test

	$\hat{\bar{\rho}}$	CD-statistic	$\hat{\alpha}$	$\hat{\sigma}_{\hat{\alpha}}$
Pre-crisis	0.964	91.415	0.7559	0.0213
Post-crisis	0.945	133.355	0.8463	0.0258
COVID-19	0.918	63.409	0.9013	0.0499

Notes: This table reports the estimated average sample correlation between local country i and j, $\hat{\bar{\rho}}$, the cross-sectional test statistics, $CD - statistics$, as well as $\hat{\alpha}$ and its standard error, $\hat{\sigma}_{\hat{\alpha}}$

4.2. Interconnection matrices and their signs

We now proceed to the analysis of the estimated weights. As described in Subsection 3.2, we computed the weights by estimating (18) via OLS. The weights describe the contribution of each $j \neq i$ to the space of the residual unexplained cross sectional variance that is unspanned by country i's sovereign yields, as in Bernanke et al. (2005).

In Tables 3 to 5, we report the weights, row normalized. Therefore, each row i features the tightness and the sign of the interconnection among country i and the foreign counterparts

[6] In the empirical application, we estimate α as in Bailey et al. (2016b)

Table 2: First Principal Component: loadings

	Pre-ESD	Post-ESD	COVID
Austria	0.321	-0.319	-0.324
Belgium	0.322	-0.371	-0.335
Finland	0.309	-0.154	-0.315
France	0.320	-0.342	-0.322
Ireland	0.312	-0.361	-0.315
Italy	0.324	-0.296	-0.294
The Netherlands	0.320	-0.314	-0.327
Portugal	0.317	-0.335	-0.326
Spain	0.324	-0.363	-0.318
Greece	0.291	-0.242	-0.281
Variance explained	0.922	0.676	0.851

Notes: This table reports the factor loadings of the first static Principal Component over the three periods of investigation and the portion of cross sectional variance explained.

j. By looking at the values, we can easily notice the presence of sign heterogeneity, some weights being positive, while others negative. This feature corresponds to the first signal of the presence of asymmetric interconnection. Specifically, already during the pre-ESD crisis period it was clear the distinction that emerged afterwords in the academic and public debate between Core and Peripheral countries. The sovereign yields of Spain, Italy, Portugal, and Greece feature an opposite sign for almost all specifications compared with Austria, Belgium, Finland, France, and The Netherlands. Such a result portraits the "flight-to-quality" phenomenon from Peripheral to Core European countries already before the outburst of the ESD crisis.

During the post-ESD crisis period, while Portugal and Greece continue to exhibit the above mentioned features, we can see mixed signs for Ireland and Italy. This result points out at the convergence path started by European countries after the introduction of unconventional monetary policies inside the euro area.

By closely looking at the COVID period of our sample, we can clearly see that the same signs of fragility are back in the sovereign bond market. As a matter of fact, the blocks of countries exhibiting opposite signs are again Core and Peripherals, with the exception of

Belgium, showing some similarities with Peripheral countries.

Table 3: Pre-*ESD* crisis period: W matrix

	AU	BE	FN	FR	IR	IT	NL	PT	SP	GR
AU	·	-0.067	-0.258	-0.138	0.035	-0.071	-0.178	0.066	0.089	0.098
BE	-0.037	·	-0.263	-0.158	0.040	-0.088	-0.169	0.060	0.084	0.101
FN	-0.023	-0.083	·	-0.161	0.037	-0.164	-0.233	0.059	0.130	0.110
FR	-0.044	-0.107	-0.275	·	0.036	-0.093	-0.172	0.058	0.106	0.111
IR	-0.056	-0.138	-0.261	-0.089	·	0.002	-0.168	0.085	0.109	0.092
IT	-0.050	-0.086	-0.297	-0.164	0.036	·	-0.132	0.053	0.093	0.089
NL	-0.046	-0.075	-0.298	-0.161	0.039	-0.111	·	0.050	0.104	0.115
PT	-0.086	-0.101	-0.344	-0.071	0.031	0.045	-0.153	·	0.053	0.116
SP	-0.074	-0.078	-0.290	-0.122	0.038	0.006	-0.196	0.096	·	0.099
GR	-0.072	-0.097	-0.205	-0.080	0.022	0.086	-0.224	0.127	0.088	·

Notes: This table reports the weights w_{ij} extracted as indicated in (A.8).

Table 4: Post-*ESD* crisis period: W matrix

	AU	BE	FN	FR	IR	IT	NL	PT	SP	GR
AU	·	-0.091	-0.683	0.052	0.0002	-0.015	-0.088	0.023	0.031	0.017
BE	-0.215	·	-0.509	0.098	-0.035	0.00003	-0.085	0.010	0.033	0.016
FN	-0.227	0.115	·	-0.092	0.048	-0.065	-0.394	0.013	0.023	0.022
FR	-0.211	-0.063	-0.511	·	-0.057	0.014	-0.061	0.019	0.047	0.017
IR	-0.137	-0.227	-0.360	0.200	·	0.017	0.030	0.007	-0.008	0.014
IT	-0.162	-0.026	-0.478	0.108	-0.026	·	-0.137	0.007	0.044	0.012
NL	-0.172	-0.070	-0.557	0.107	-0.025	-0.006	·	0.013	0.035	0.016
PT	-0.176	-0.209	-0.317	0.169	-0.039	0.025	0.033	·	0.018	0.014
SP	-0.158	-0.180	-0.390	0.187	-0.026	0.017	0.021	0.007	·	0.015
GR	-0.124	-0.219	-0.272	0.209	-0.050	0.022	0.049	0.010	0.044	·

Notes: This table reports the weights w_{ij} extracted as indicated in (A.8).

4.3. Impulse response analysis

After the analysis of the transmission matrix W, we evaluate the properties of the $GVAR$ model as expressed in (17) by studying the impulse response functions. Their analysis can provide useful insights when we study a multivariate dynamic systems. In particular, the impulse response functions map the responses of the system to the effect of shocking one of

Table 5: COVID period: W matrix

	AU	BE	FN	FR	IR	IT	NL	PT	SP	GR
AU	·	0.026	-0.140	-0.377	0.058	0.063	-0.124	0.040	-0.126	0.047
BE	-0.177	·	-0.107	-0.256	0.068	0.061	-0.210	-0.002	-0.067	0.050
FN	-0.213	0.027	·	-0.317	0.063	0.060	-0.147	0.025	-0.102	0.047
FR	-0.282	0.111	-0.156	·	0.040	0.038	0.007	0.079	-0.232	0.056
IR	-0.165	-0.050	-0.101	-0.174	·	0.066	-0.331	-0.042	-0.013	0.058
IT	-0.192	-0.078	-0.051	0.062	0.068	·	-0.338	-0.093	0.064	0.054
NL	-0.176	0.028	-0.124	-0.344	0.064	0.065	·	0.033	-0.117	0.049
PT	-0.181	-0.002	-0.110	-0.262	0.068	0.061	-0.199	·	-0.067	0.050
SP	-0.143	0.046	-0.142	-0.481	0.042	0.059	-0.015	-0.020	·	0.052
GR	-0.124	-0.090	-0.032	-0.082	0.092	0.069	-0.425	-0.046	0.040	·

Notes: This table reports the weights w_{ij} extracted as indicated in (A.8).

the variables at different horizons. For example, we could be interested in the response of the Italian $10Y$ spreads to a 200 basis points shock on the Greek $10Y$ spread.

In our framework, we have three channels of transmissions of a shock from country i to j: a) via the contemporaneous factor $\hat{F}_{2,t}$, b) its lag $\hat{F}_{2,t-1}$ and c) via the covariance matrix of the errors. Instead of employing the original shocks, the traditional VAR literature opts for Orthogonalized Impulse Responses (OIR) (Sims, 1980) or restrictions on the covariance matrix (Bernanke, 1986; Sims, 1986; Blanchard and Quah, 1989) to identify structural shocks. However, it is difficult to have a clear identification strategy in a $GVAR$ framework both when choosing the relevant restrictions in the covariance matrix of the Global VAR and when deciding the order of countries and variables in the OIR set up. The Generalized Impulse Response ($GIRF$) is an alternative method that is invariant to the ordering of the variables and the countries in the $GVAR$ (Pesaran and Shin, 1998; Pesaran et al., 1999) and does not require any restrictions on the covariance matrix of the residuals. In our framework, the $GIRF$ consists of inducing a one-period shock only on one variable, e.g., the $10Y$ spread of country i, and then, ruling out the historically observed distribution of the errors, predicting the effect of such shock on the system at different horizons.

In the following subsections, we present the generalized impulse response functions in the

pre- and post-ESD crisis with a supplementary focus on the COVID pandemic. We build the confidence interval using $10,000$ bootstrap replications (see Appendix A for more details), indicating with a red solid line the median response and with black dotted lines the 16^{th} and 84^{th} confidence bounds.

4.4. Pre-ESD crisis period

Figure 2 reports the generalized impulse responses to a 200 basis points (b.p.) shock to the Spanish $10Y$ differentials. Spain was selected as it is a large Peripheral country, which has been quite affected during the ESD crisis period but also by the COVID pandemic.[7]

First, despite this sub sample precedes the ESD crisis period, our model shows that signs of fragmentation of euro area into Core and Periphery was already taking place before the beginning of the European sovereign debt crisis. On the one hand, Italy, Ireland, Portugal and Greece are impacted in a similar manner by a 200 b.p. shock to Spain, their differentials are all expected to increase.

Beside the sign, the size of such effect is also relevant: the estimated impact is well beyond 60 b.p., (150 b.p. for Greece) with the only exception being Portugal. However, the impact of Portuguese differential is not statistically significant up to two weeks horizon, but then the expected increase of the spread becomes significant and particularly persistent.

On the other hand, with the exception of Belgium, Core economies' differentials are expected to significantly decrease: this is a first sign of the "flight-to-quality" mechanism that would be typically studied in the context of the European Sovereign Debt crisis. A second important aspect that will be a common feature of our results is the humped shape of the $GIRF$. In fact, while the first transmission of the shock occurs at the level of the covariance matrix of the $GVAR$, then subsequent effects and the persistence of the impact are mostly due to the *foreign* factor and its lag. The case of Belgium is exemplary of this: despite a first

[7]Italy for example has been less affected in term of GDP by the recent pandemic. We refer to the Supplementary Material for the $GIRF$s to a 200 b.p. shock to the remaining Peripheral countries.

significant increase of its differential with respect to Germany (a stylized fact also underlined by Candelon and Luisi, 2020), the $10Y$ spread's response becomes insignificant, dropping in the mild negative territory, aligning Belgium to the other Core economies.

Pre-*ESD* crisis

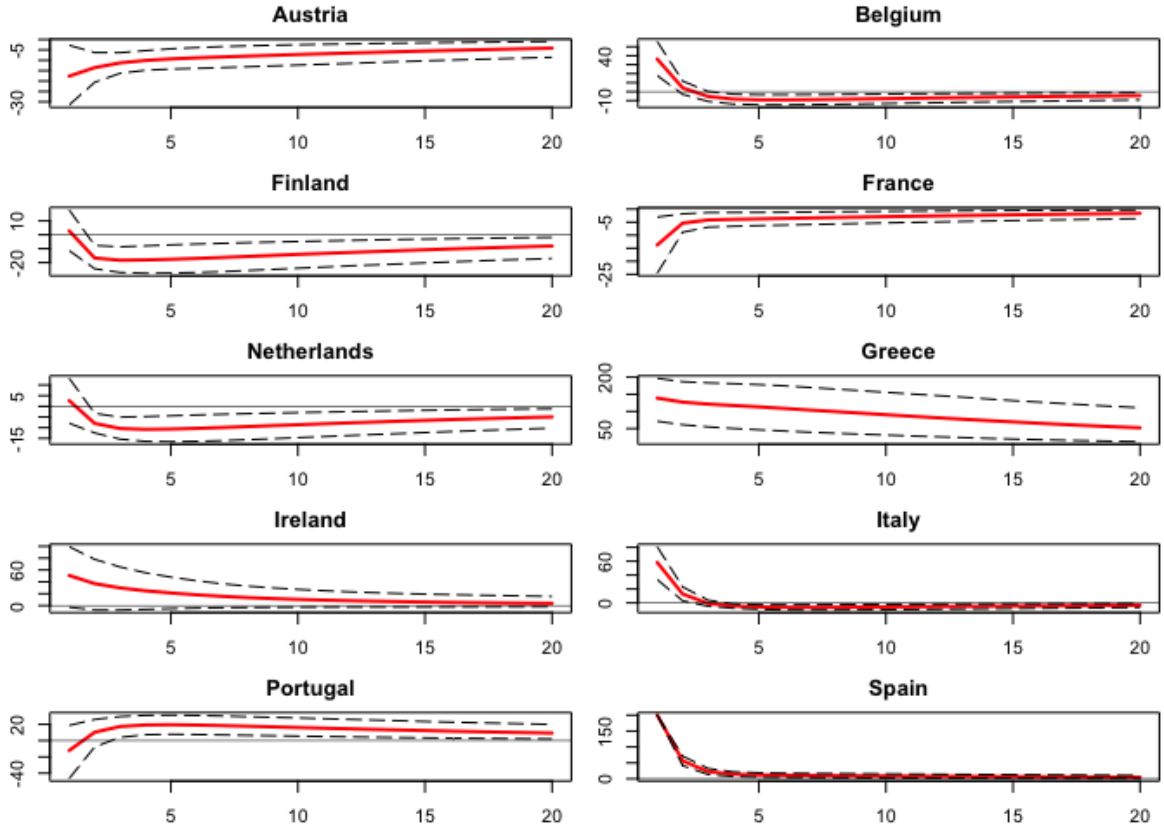

Figure 2: The figure reports the Generalized Impulse Response Functions to a 200 b.p. shock to the $10Y$ Spanish Spread in the pre-crisis period. $[16^{th}, 84^{th}]$ confidence intervals are calculated using $10,000$ bootstrap replications as described in Appendix A.

4.5. Post-ESD crisis period

Figure 3 reports the generalized impulse responses to a 200 basis points (b.p.) shock to the Spanish spread. Compared to the pre-ESD crisis period, some differences are worth to be underlined. The shock to the Spanish differentials is expected to induce a generalized statistically significant increase on the spreads of both Peripheral and Core economies: there are no signals of a "flight-to-quality" mechanism. Nevertheless, there is still a marked difference in the size of the impact: while the response of the Core economies is particularly contained

in size, the impact of the same shock on the other Peripheral country remains important (e.g., over 150 b.p. for Greece) and persistent. Figure 3 depicts a picture where, despite the unconventional monetary policies of the ECB, and the $OMTs$ in particular, have neutralized the perception of the risk of a break up of the euro area, markets still acknowledge the financial fragility of the Periphery relative to the Core.

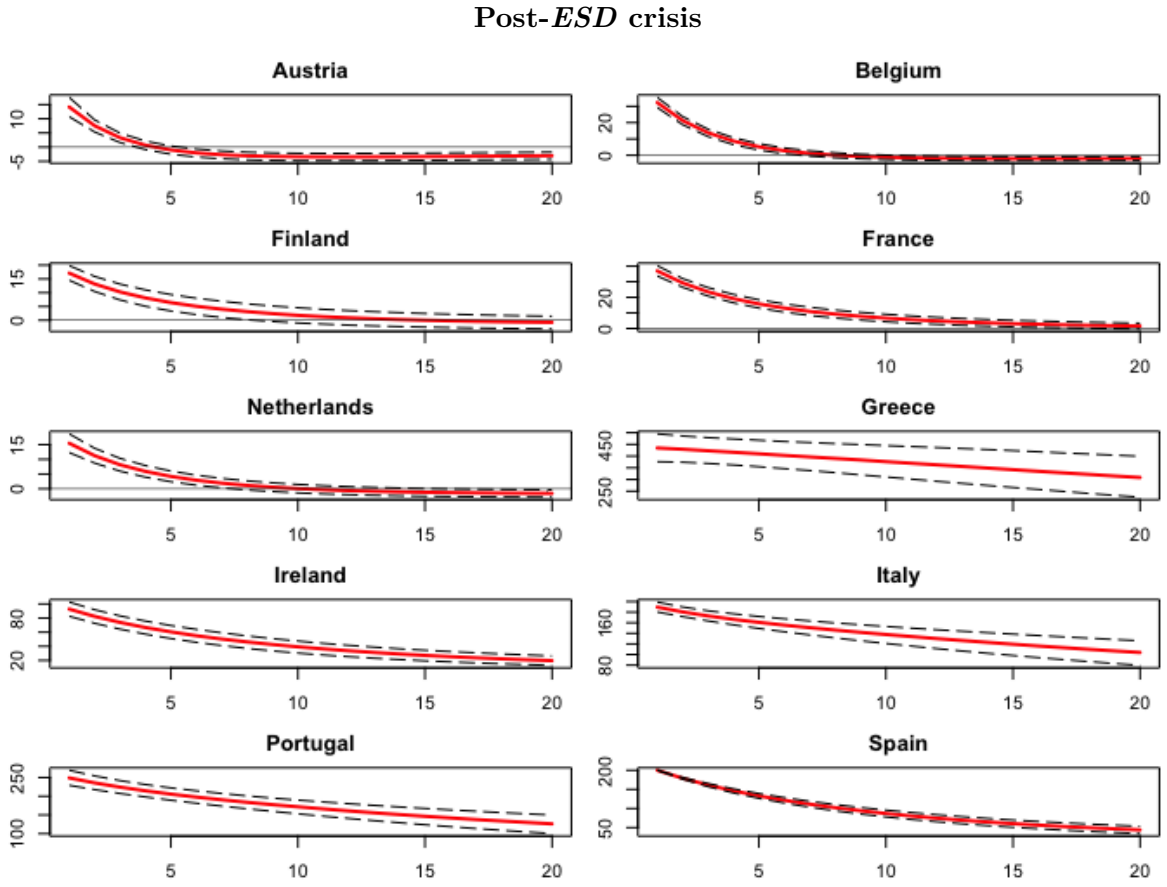

Figure 3: The figure reports the Generalized Impulse Response Functions to a 200 b.p. shock to the $10Y$ Spanish Spread in the post-crisis period. $[16^{th}, 84^{th}]$ confidence intervals are calculated using $10,000$ bootstrap replications as described in Appendix A.

4.6. The COVID pandemic period 2019 *March* - 2021 *March*

As in the previous analyses of the $GIRF$s, we still consider a 200 b.p. shock to the Spanish spreads also in Figure 4.

A question that naturally arises from the analysis of Figure 4 is whether the convergence phase that followed the unconventional monetary policy measures and, in particular the

$OMTs$ announcement, is over. In fact, while the size of the responses to 200 b.p. shock to Spain of the Peripheral economies remains somehow unchanged compared to the post-ESD crisis period, Figure 4 depicts a completely different picture compared to Figure 3 with respect the responses of the Core economies: the shock to the $10Y$ Spanish differentials also induces a generalized and statistically significant decrease in the $10Y$ differentials in Core economies. This result highlights the revival of flight-to-quality effect, leading to an increase in the potential risk of fragmentation of the euro area.

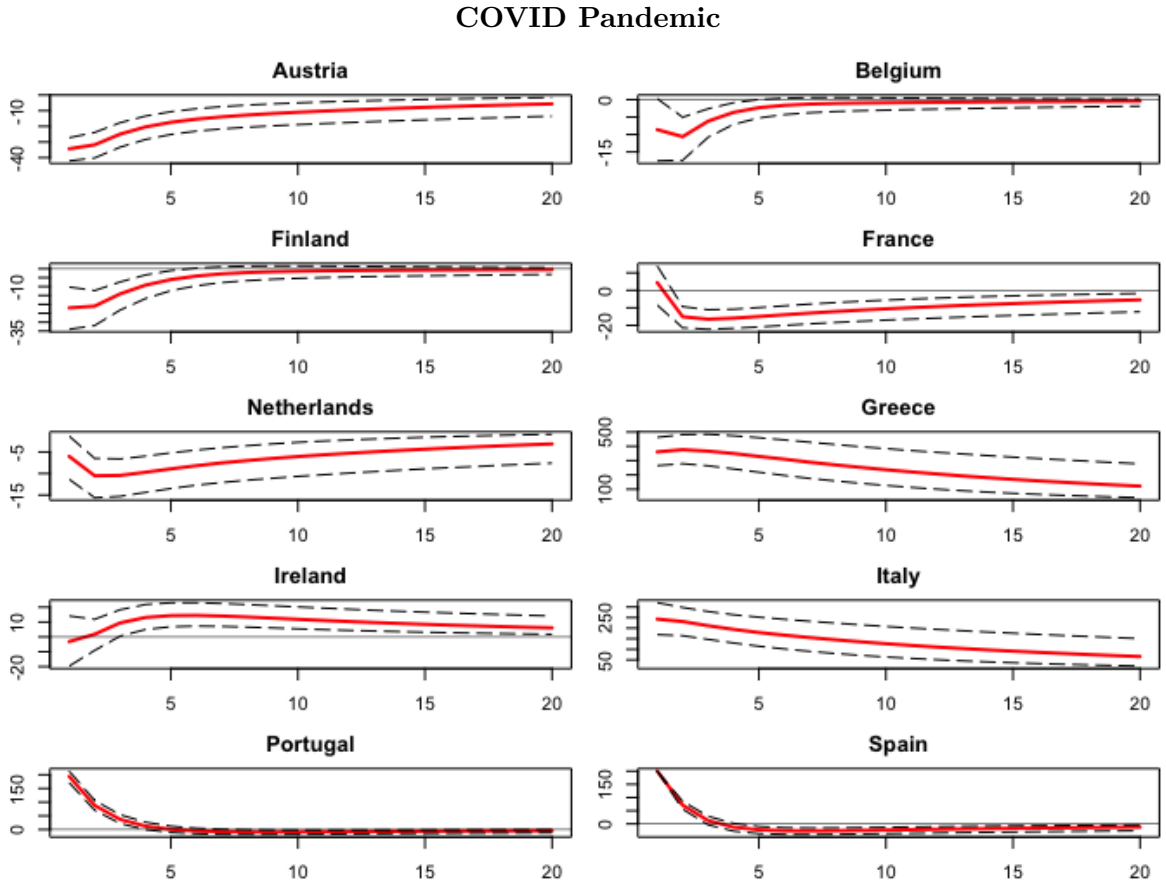

Figure 4: The figure reports the Generalized Impulse Response Functions to a 200 b.p. shock to the $10Y$ Spanish Spread in the COVID period. $[16^{th}, 84^{th}]$ confidence intervals are calculated using $10,000$ bootstrap replications as described in Appendix A.

4.7. Heatmap: a closer look at the interconnections underlying the GIRFs

To summarize the message conveyed by $GIRF$s, we have reported in Figure 5 the heatmap defined by the average correlations of the different $GIRF$ after a 200 basis points (b.p.) shock to the Greek, Irish, Italian, Portuguese and Spanish $10Y$ differentials.

We hence focus on the signs of the responses to a shock in a Peripheral country. To this goal, the heatmap is built on the correlation between the different $GIRF$s obtained after a shock in the spread of a Peripheral country for a given forecasting horizon. In our case, we consider a 30 weeks forecasting horizon and the three selected periods: pre-ESD crisis, post-ESD crisis and the COVID pandemic.

Heatmap representation of the Generalized Impulse Response Functions

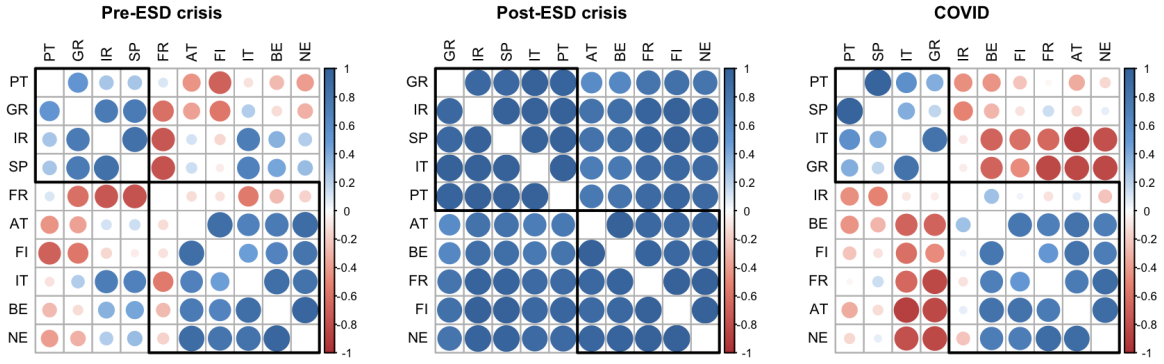

Figure 5: The figure displays the average heatmap representation of the Generalized Impulse Response Functions to a 200 b.p. shock to the $10Y$ Greek, Spanish, Portuguese and Italian Spreads in the pre-crisis, post crisis and COVID pandemic period with a 30 weeks forecasting horizon. We indicate in blue and red, the positive or negative sign of the correlation between two countries, respectively. The shade of the color and the diameter of the circle represents the intensity of the correlation: the darker (the greater) the circle is, the stronger the correlation is. The rectangles identify the clusters defined by the dissimilarity measure $1-\rho_{i,j}$, with $\rho_{i,j}$ being the pairwise average correlation coefficient between the GIRF of country i and j to a 200 b.p. shock to Greece, Ireland, Italy, Portugal and Spain.

The fragmentation between Core and Peripheral European countries is evident in the pre-ESD crisis period. Ireland, Italy, Greece, Spain and Portugal are strongly and positively correlated together but they are also negatively (or weakly) correlated to the Core European countries. As the sample ends before the ignition of the ESD crisis, this finding confirms the good predictive power of our $GVAR$ model with positive and negative weights in the transmission matrix W. Two countries appear to have a specific role. On the one hand, France is weakly negatively correlated to both Peripheral and other Core countries. On the other hand, Italy is the important node as it constitutes the junction between both groups: it is positively correlated to Ireland, Greece and Spain but also positively correlated to Austria, Finland, Belgium and Netherlands. This strategic positioning reveals the key role played in the fragmentation risk by this country.

The post-ESD crisis heatmap shows that all the measures enhanced by the ECB have

successfully neutralized the devaluation risk and created tighter links between European sovereign bonds. Furthermore, the signs of the interconnections are all strongly positive: this further underlines how, in this period, the euro area sovereign debts behaved as an integrated market.

The COVID period heatmap surprisingly looks similar to the pre-ESD crisis one. The degree of similarity amounts to 51.71%, which is well above 0 and quite high when comparing with the post-ESD crisis period (11.70%).[8] Both groups, Core and Peripheral Europe, are once again fragmented. Only three slight differences with the pre-ESD crisis can be noticed: first, while Italy joins the group of Peripheral countries, Ireland becomes more positively (or weakly) correlated to the Core economies, hence leaving the periphery. Second, France is reintegrating its positioning in the European Core group. The similarities of the pre-ESD crisis and the COVID periods constitute therefore a clear signal for a rehearsal of the fragmentation risk in the European union. Structural vulnerabilities are again present and strong, confirming the conclusions of the recent Global Financial Stability Report ($GFSR$, April 2021) of the International Monetary Fund.

5. Conclusion

This paper sheds new light on the fragmentation risk in the European Monetary Union. A novel methodology reconciling Factor augmented and $GVAR$ models allows to disentangle interdependence from "contagion" and "flight-to-quality". It is implemented for yield spreads between 10 year euro area government bonds and the German safe benchmark over three remarkable periods: The pre-ESD crisis, the post-ESD crisis as well as the recent COVID period. It appears that signs of "contagion" and "flight-to-quality" effects were al-

[8]We compute the degree of similarity between the heatmaps by the percentage average L1 norm of the difference between the correlation matrices underlying the heatmap representations in the pre-, post-ESD crisis and COVID periods.

ready present in the pre-ESD crisis period, pointing out at latent fragmentation risk between Southern European countries (Portugal, Italy, Ireland, Greece and Spain) and the Northern ones. Soon after the ESD crisis, the different programs of public bonds purchases implemented by the European Central Banks have limited this risk, leading all European spreads to shrink homogeneously. The COVID pandemic has reintroduced the fragmentation risk at the forefront of the European sovereign bond market for Southern European countries. Contrary to the pre-ESD crisis period, our findings show that an asymmetric local shock could transmit heterogeneously over countries, even if they share the same currency. It therefore rejoins the recent articles pointing the same heterogeneity regarding the effects of monetary policies as Corsetti et al. (2020).

The rise of the fragmentation risk in Europe and the heterogeneous transmission of common policy constitute then a challenge for European authorities. It also signals that the re-integration process of euro area government bonds is very fragile despite the huge and unprecedented amount of monetary stimulus put in place (see Borgioli et al., 2020). Given the positive results obtained in the post-ESD crisis period, it appears relevant to continue in this direction. Among the solutions, an extension of the Quantitative Easing could be considered, even if it would rapidly encounter the constraint of the shares of different national central banks in the ECB's capital, as well as the uncertain timing of the pandemics (Demertzis, 2020). The monetary stimulus should therefore be completed by deeper fiscal integration. The common recovery plan, leading to the issuance of European mutualized debt is a first step towards this direction. It is nevertheless rather limited in the amount (at the moment around 2% of the national public debt), and in any case should be accompanied by public spending monitoring in order to enhance economic convergence across European countries. A decrease in the fragmentation risk appears therefore difficult in the short-run but is mandatory to avoid another sovereign debt crisis.

References

Baele, L., Ferrando, A., Hördahl, P., Krylova, E., and Monnet, C. (2004), "Measuring European financial integration," *Oxford Review of Economic Policy*, 20, pp. 509–530.

Bailey, N., Holly, S., and Pesaran, M. H. (2016a), "A two-stage approach to spatio-temporal analysis with strong and weak cross-sectional dependence," *Journal of Applied Econometrics*, 31, pp. 249–280.

Bailey, N., Kapetanios, G., and Pesaran, M. H. (2016b), "Exponent of cross-sectional dependence: Estimation and inference," *Journal of Applied Econometrics*, 31, pp. 929–960.

Balabanova, Z., and Brüggemann, R. (2017), "External information and monetary policy transmission in new EU member states: results from FAVAR models," *Macroeconomic Dynamics*, 21, pp. 311–335.

Bernanke, B. S. (1986), "Alternative explanations of the money-income correlation," *Carnegie-Rochester Conference Series on Public Policy*, 25, pp. 49–99.

Bernanke, B. S., Boivin, J., and Eliasz, P. (2005), "Measuring the effects of monetary policy: a factor-augmented vector autoregressive (FAVAR) approach," *The Quarterly journal of economics*, 120, pp. 387–422.

Blanchard, O. J., and Quah, D. (1989), "The Dynamic Effects of Aggregate Demand and Supply Disturbances," *American Economic Review*, 79, pp. 655–673.

Borgioli, S., Horn, C., Kochanska, U., Molitor, P., and Mongelli, S. (2020), "European financial integration during the covid-19 crisis," *ECB Economic Bulletin*.

Candelon, B., and Luisi, A. (2020), "Testing for the Validity of W in GVAR models," Tech. rep., Université catholique de Louvain, Louvain Finance (LFIN).

Candelon, B., and Tokpavi, S. (2016), "A non-parametric test for Granger-causality in distribution with application to financial contagion," *Journal of Business & Economic Statistics*, 34, pp. 240–253.

Cole, H. L., and Kehoe, T. J. (2000), "Self-fulfilling debt crises," *The Review of Economic Studies*, 67, pp. 91–116.

Corsetti, G., and Dedola, L. (2016), "The Mystery of the Printing Press: Monetary Policy and Self-Fulfilling Debt Crises," *Journal of the European Economic Association*, 14, pp. 1329–1371.

Corsetti, G., Duarte, J. B., and Mann, S. (2020), "The heterogeneous transmission of ecb policies: Lessons for a post-covid europe," *VoxEu*.

Corsetti, G., Kuester, K., Meier, A., and Muller, G. J. (2014), "Sovereign risk and belief-driven fluctuations in the euro area," *Journal of Monetary Economics*, 61, pp. 53–73.

De Grauwe, P., and Ji, Y. (2012), "Mispricing of sovereign risk and macroeconomic stability in the eurozone," *Journal of Common Market Studies*, 50, pp. 866–880.

De Santis, R. (2019), "Redenomination risk," *Journal of Money, Credit and Banking*, 51, pp. 2173–2206.

Dees, S., Mauro, F. d., Pesaran, M. H., and Smith, L. V. (2007), "Exploring the international linkages of the euro area: a global VAR analysis," *Journal of Applied Econometrics*, 22, pp. 1–38.

Demertzis, M. (2020), "Monetary policy in the time of covid-19, or how uncertainty is here to stay," *Monetary Dialogue Papers*.

Elhorst, J. P., Gross, M., and Tereanu, E. (2020), "Cross-sectional dependence and spillovers in space and time: where spatial econometrics and global VAR models meet," *Journal of Economic Surveys*.

Favero, C., and Missale, A. (2012), "Sovereign spreads in the eurozone: which prospects for a Eurobond?" *Economic Policy*, 27, pp. 231–273.

Favero, C., Pagano, M., and Von Thadden, E.-L. (2010), "How does liquidity affect government bond yields?" *Journal of Financial and Quantitative Analysis*, 45, pp. 107–134.

Favero, C. A. (2013), "Modelling and forecasting government bond spreads in the euro area: a GVAR model," *Journal of Econometrics*, 177, pp. 343–356.

Favero, C. A., and Missale, A. (2016), "Contagion in the EMU–the role of Eurobonds with OMTs," *Review of Law & Economics*, 12, pp. 555–584.

Forbes, K. J., and Rigobon, R. (2002), "No contagion, only interdependence: measuring stock market comovements," *The Journal of Finance*, 57, pp. 2223–2261.

Georgoutsos, D. A., and Migiakis, P. M. (2013), "Heterogeneity of the determinants of euro-area sovereign bond spreads; what does it tell us about financial stability?" *Journal of Banking & Finance*, 37, pp. 4650–4664.

Gross, M. (2019), "Estimating GVAR weight matrices," *Spatial Economic Analysis*, 14, pp. 219–240.

Harbo, I., Johansen, S., Nielsen, B., and Rahbek, A. (1998), "Asymptotic inference on cointegrating rank in partial systems," *Journal of Business & Economic Statistics*, 16, pp. 388–399.

House, C. L., Proebsting, C., and Tesar, L. L. (2020), "Austerity in the aftermath of the great recession," *Journal of Monetary Economics*, 115, pp. 37–63.

Kilian, L. (1998), "Small-sample confidence intervals for impulse response functions," *Review of Economics and Statistics*, 80, pp. 218–230.

Mammen, E. (1993), "Bootstrap and wild bootstrap for high dimensional linear models," *The Annals of Statistics*, pp. 255–285.

Metiu, N. (2012), "Sovereign risk contagion in the eurozone," *Economics Letters*, 117, pp. 35–38.

Monfort, A., and Renne, J.-P. (2013), "Decomposing euro-area sovereign spreads: credit and liquidity risks," *Review of Finance*, 18, pp. 2103–2151.

Pesaran, M., and Shin, Y. (1998), "Generalized impulse response analysis in linear multivariate models," *Economics Letters*, 58, pp. 17–29.

Pesaran, M. H. (2021), "General diagnostic tests for cross-sectional dependence in panels," *Empirical Economics*, 60, pp. 13–50.

Pesaran, M. H., Schuermann, T., and Weiner, S. M. (2004), "Modeling regional interdependencies using a global error-correcting macroeconometric model," *Journal of Business & Economic Statistics*, 22, pp. 129–162.

Pesaran, M. H., Shin, Y., and Smith, R. P. (1999), "Pooled mean group estimation of dynamic heterogeneous panels," *Journal of the American Statistical Association*, 94, pp. 621–634.

Sgherri, S., and Zoli, E. (2009), "Euro area risk during the crisis," *International Monetary Fund Working Paper 09/222*.

Sims, C. A. (1980), "Macroeconomics and reality," *Econometrica*, 48, pp. 1–48.

——— (1986), "Are forecasting models usable for policy analysis?" *Quarterly Review*, 10, pp. 2–16.

Stock, J. H., and Watson, M. W. (2016), *Dynamic factor models, factor-augmented vector autoregressions, and structural vector autoregressions in macroeconomics*, vol. 2, Elsevier.

Vega, S. H., and Elhorst, J. P. (2016), "A regional unemployment model simultaneously accounting for serial dynamics, spatial dependence and common factors," *Regional Science and Urban Economics*, 60, pp. 85–95.

Appendix A. Bootstrap procedure for the GIRF confidence bounds

The advantages of the bootstrapping procedure when computing confidence intervals for impulse responses in the VAR framework are described in Kilian (1998). In our framework, to take into account also unknown forms of heteroskedasticity, we proposed the wild bootstrapped procedure as in Mammen (1993). Specifically,

1. Estimate the local $VARX^*$ parameters in eq. (17) (after retrieving the weights as outlined in Appendix B), and the corresponding residuals u_t^i for each $i = 1, \ldots, N$

2. Following the procedure outlined in Section 3.1, simultaneously solve the model to get the global VAR representation as of (15)

$$(Y_t - Y_t^{DE}) = G^{-1}H(Y_{t-1} - Y_{t-1}^{DE}) + G^{-1}u_t \tag{A.1}$$

with

$$(Y_t - Y_t^{DE}) = ((Y_t^1 - Y_t^{DE})', (Y_t^2 - Y_t^{DE})', \ldots, (Y_t^N - Y_t^{DE})')', \tag{A.2}$$

$$G = [I_N - (diag(\beta_{12}, \beta_{22}, \ldots, \beta_{N2})\tilde{W})], \tag{A.3}$$

$$H = [(diag(\beta_{11}, \beta_{21}, \ldots, \beta_{N1}) + (diag(\beta_{13}, \beta_{23}, \ldots, \beta_{N3})\tilde{W})], \tag{A.4}$$

$$u_t = (u_t^{1\prime}, u_t^{2\prime}, \ldots, u_t^{N\prime})' \tag{A.5}$$

3. Draw with replacement the sequence of errors $\{\tilde{u}_t\}_{t=2}^T = \{\tilde{u}_t^1, \ldots, \tilde{u}_t^N\}_{t=2}^T = \{k_t\hat{u}_t^1, \ldots, k_t\hat{u}_t^N\}_{t=2}^T$ with

$$k_t = \begin{cases} \frac{1+\sqrt{5}}{2}, & \text{with probability } p = \frac{\sqrt{5}-1}{2\sqrt{5}} \\ \frac{1-\sqrt{5}}{2}, & \text{with probability } 1-p. \end{cases}$$

as in Mammen (1993), $\tilde{u}_t$ are the stacked estimated local errors.

4. Generate the bootstrapped data sample according to equation A.1. The initial values are the actual ones, and u_t is replaced by the bootstrapped $\tilde{u}_t$.

5. Estimate the local $VARX^*$ on the bootstrapped data sample and compute the corresponding Generalized Impulse Responses

6. Repeat 3 - 5 a large number of times (in our example, we repeat the procedure $10,000$ times), and then extract the quantiles needed.

Appendix B: How to retrieve the country specific weights

Following the intuition of Bernanke et al. (2005), we employ the following methodology to extract foreign information from the second Principal Component of the cross section of spreads:

1. Extract the second Principal Component ($\hat{F}_{2,t}$) of the cross section of spreads

2. Regress the second Principal Component on the specific local spread I under analysis

$$\hat{F}_{2,t} = \gamma_i(Y_t^i - Y_t^{DE}) + \nu_{it} \tag{A.6}$$

3. Clean the second Principal Component from the information spanned by country i

$$\hat{F}_{2i,t} = \hat{F}_{2t} - [\hat{\gamma}_i(Y_t^i - Y_t^{DE})] \tag{A.7}$$

4. Obtain the external information as average of foreign spreads

5. Repeat 2 - 5 for each i.

$$\hat{F}_{2,it} = \sum_{i \neq j} w_{ij}(Y_t^j - Y_{t-1}^{DE}) + v_{it} \tag{A.8}$$

6. Estimate equation A.8 and retrieve the weights.

Supplementary Material

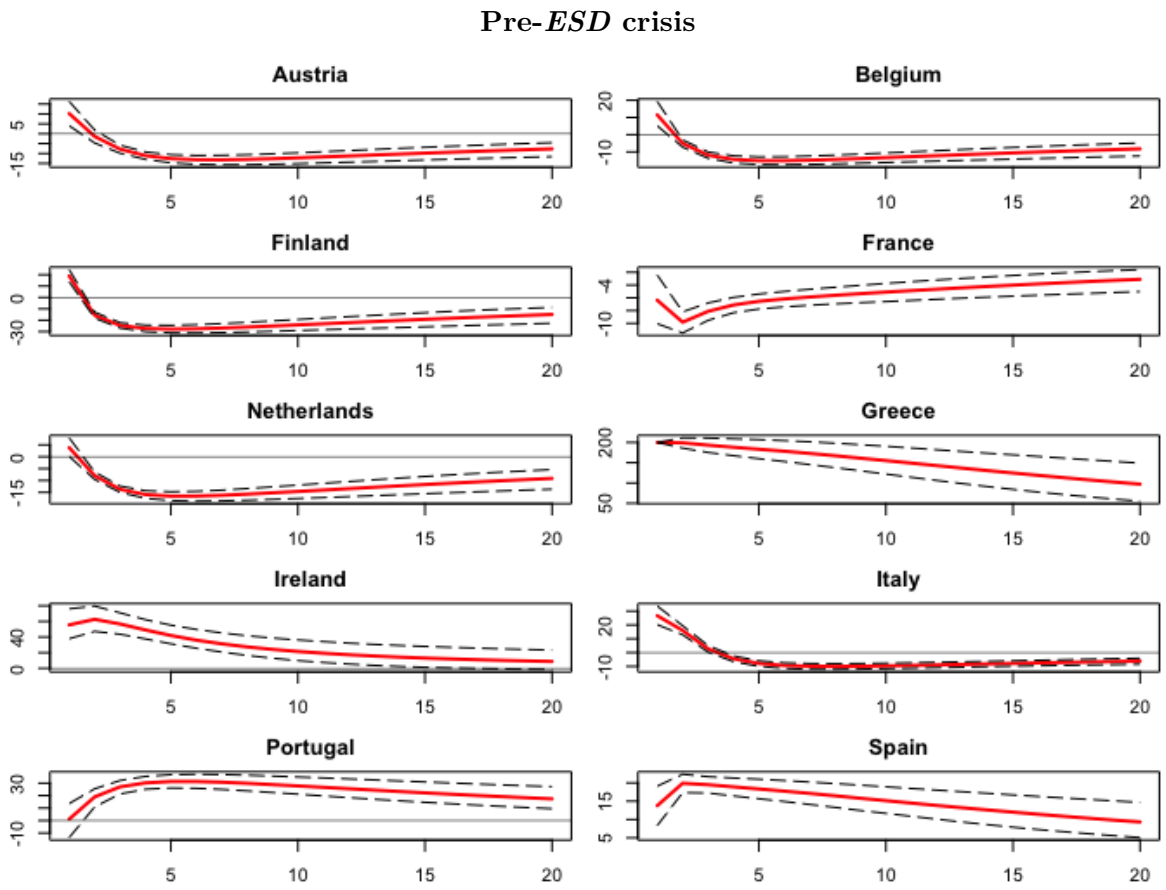

Figure A.6: The figure reports the Generalized Impulse Response Functions to a 200 b.p. shock to the $10Y$ Greek Spread in the pre-crisis period. $[16^{th}, 84^{th}]$ confidence intervals are calculated using $10,000$ bootstrap replications as in Appendix A.

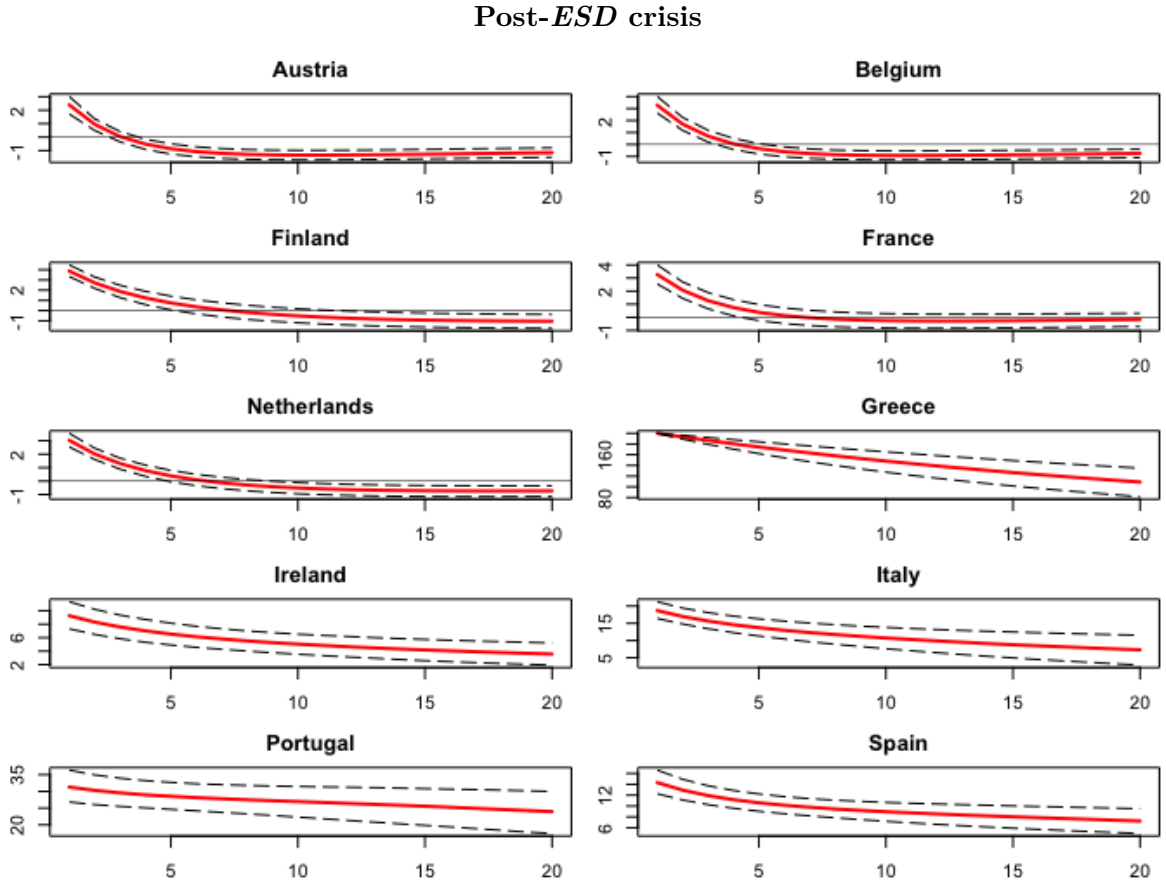

Figure A.7: The figure reports the Generalized Impulse Response Functions to a 200 b.p. shock to the $10Y$ Greek Spread in the post-crisis period. $[16^{th}, 84^{th}]$ confidence intervals are calculated using $10,000$ bootstrap replications as in Appendix A.

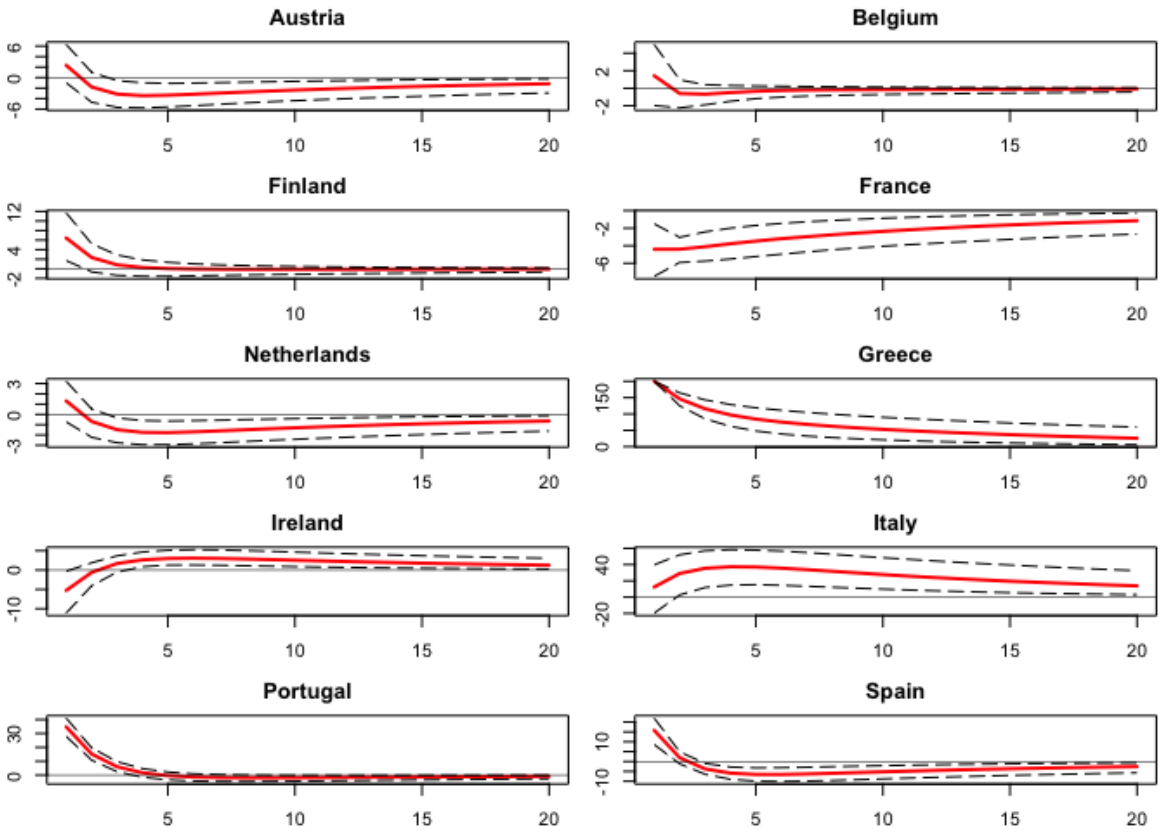

Figure A.8: The figure reports the Generalized Impulse Response Functions to a 200 b.p. shock to the $10Y$ Greek Spread in the COVID pandemic period. $[16^{th}, 84^{th}]$ confidence intervals are calculated using $10,000$ bootstrap replications as in Appendix A.

Pre-*ESD* crisis

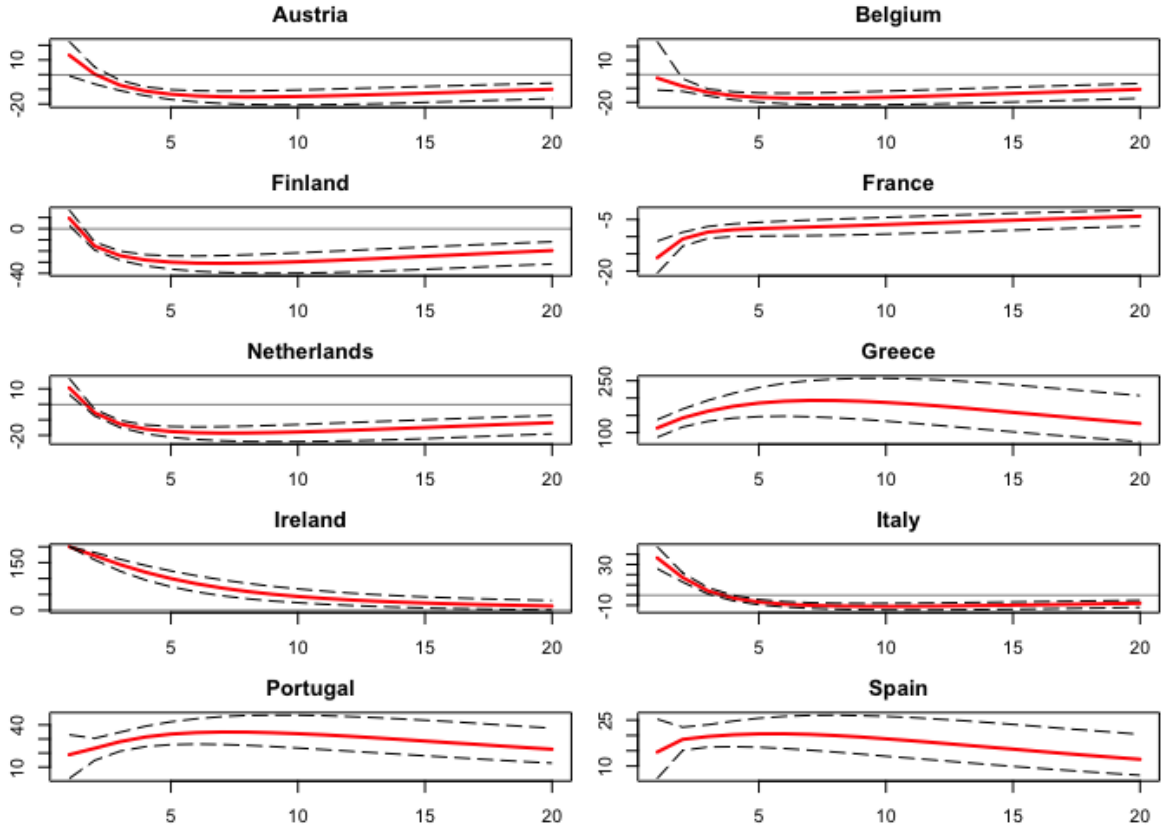

Figure A.9: The figure reports the Generalized Impulse Response Functions to a 200 b.p. shock to the $10Y$ Irish Spread in the pre-crisis period. $[16^{th}, 84^{th}]$ confidence intervals are calculated using $10,000$ bootstrap replications as in Appendix A.

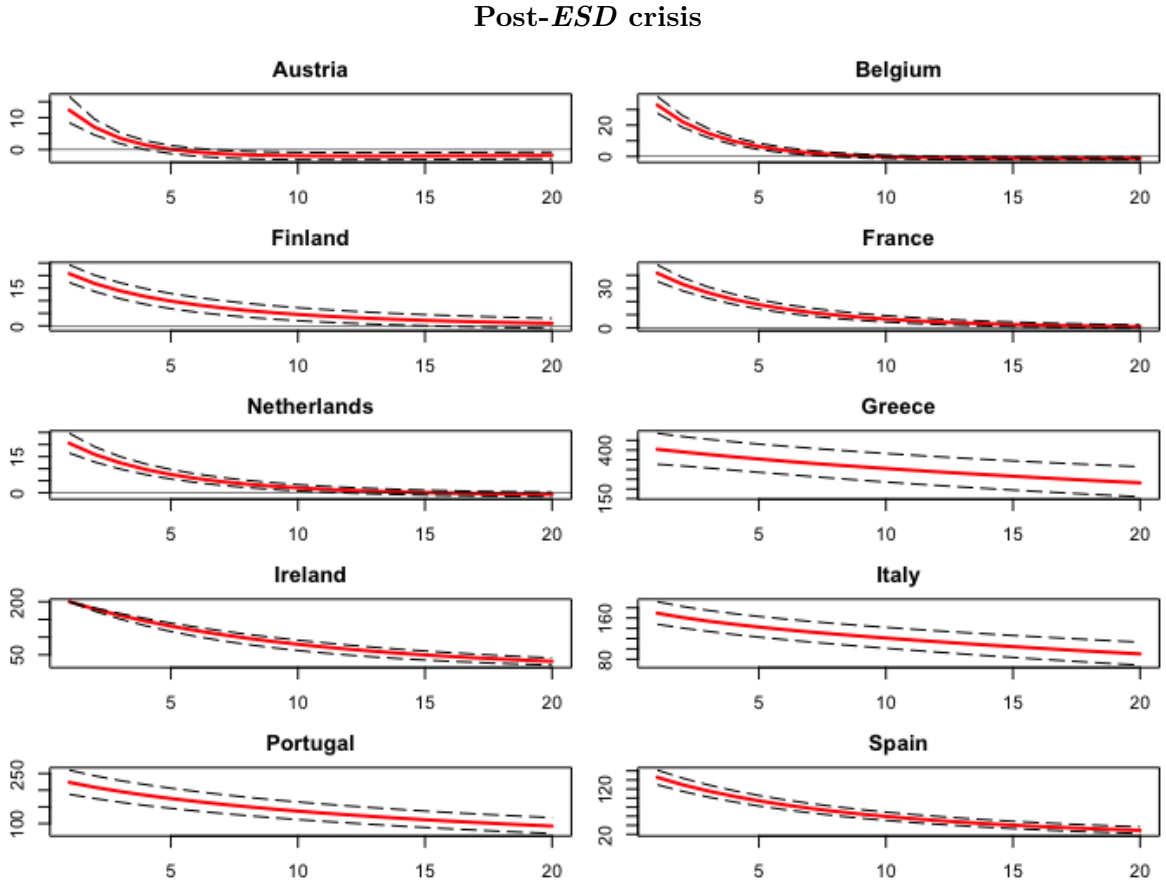

Figure A.10: The figure reports the Generalized Impulse Response Functions to a 200 b.p. shock to the $10Y$ Irish Spread in the post-crisis period. $[16^{th}, 84^{th}]$ confidence intervals are calculated using $10,000$ bootstrap replications as in Appendix A.

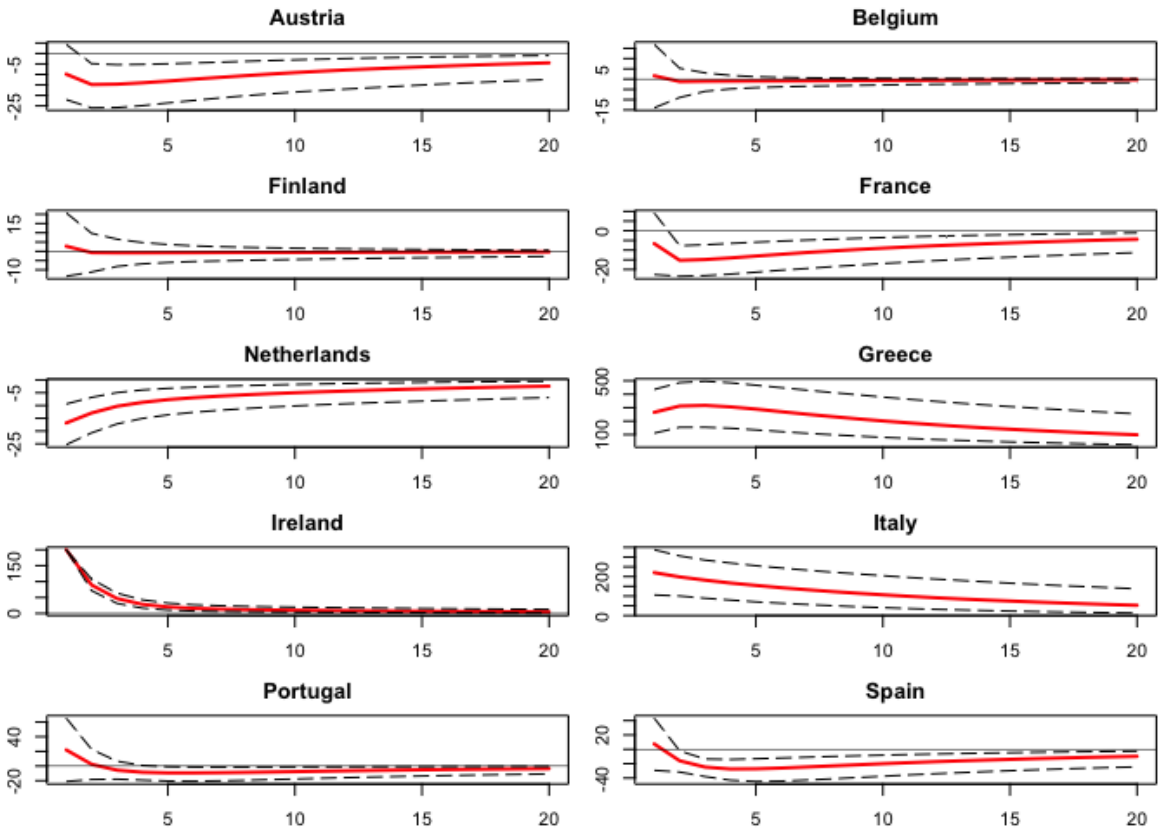

Figure A.11: The figure reports the Generalized Impulse Response Functions to a 200 b.p. shock to the $10Y$ Irish Spread in the COVID pandemic period. $[16^{th}, 84^{th}]$ confidence intervals are calculated using $10,000$ bootstrap replications as in Appendix A.

Pre-*ESD* crisis

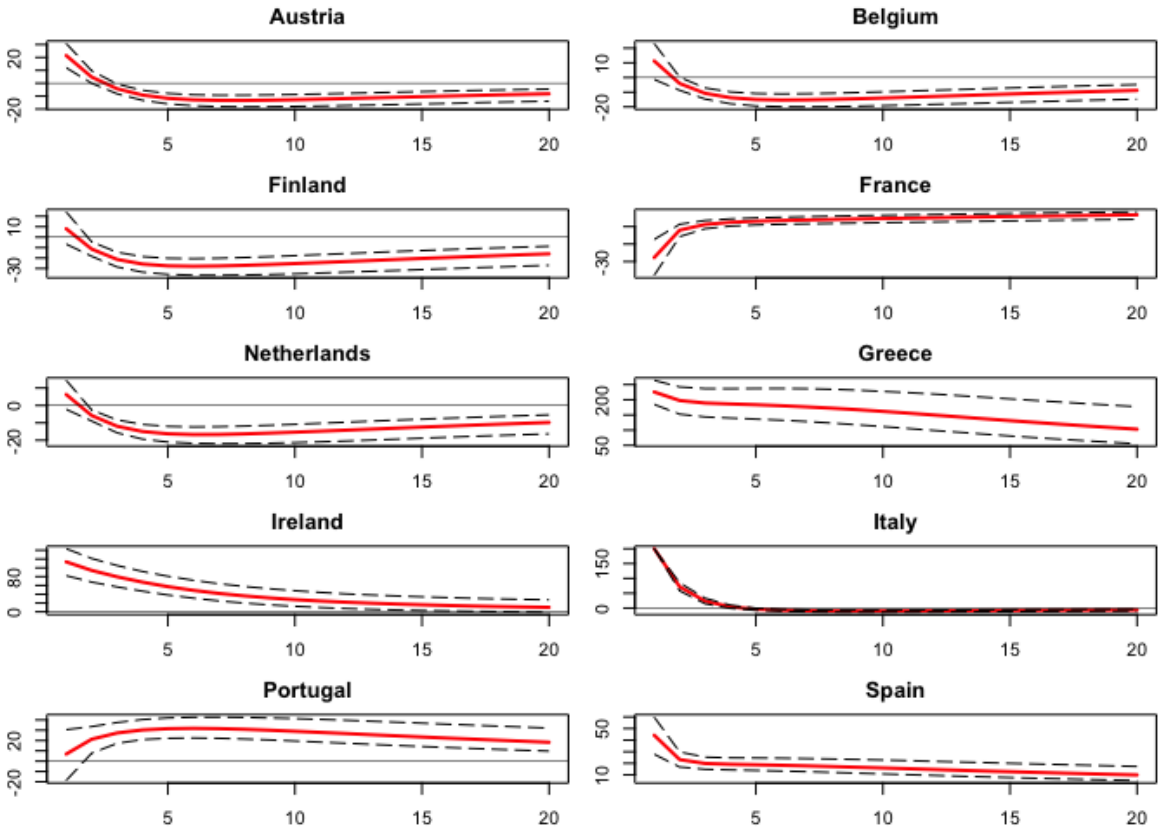

Figure A.12: The figure reports the Generalized Impulse Response Functions to a 200 b.p. shock to the $10Y$ Italian Spread in the pre-crisis period. $[16^{th}, 84^{th}]$ confidence intervals are calculated using $10,000$ bootstrap replications as in Appendix A.

Post-*ESD* crisis

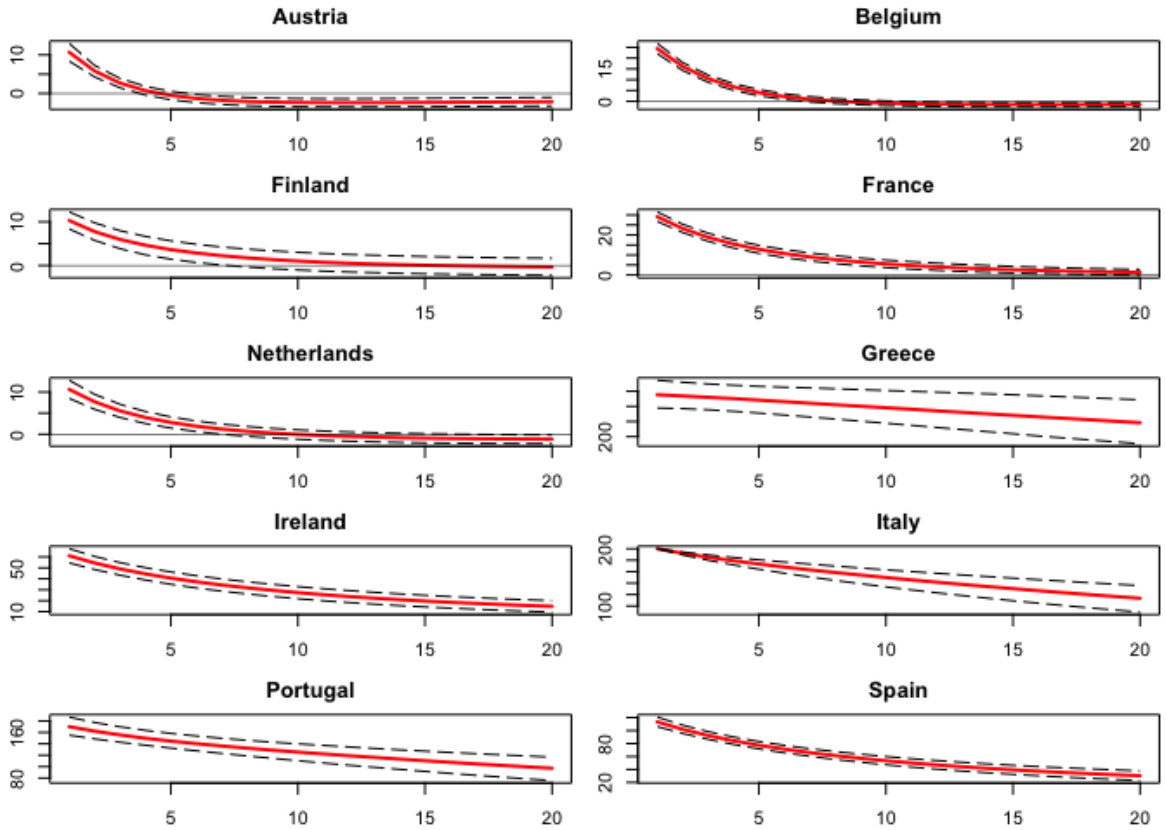

Figure A.13: The figure reports the Generalized Impulse Response Functions to a 200 b.p. shock to the $10Y$ Italian Spread in the post-crisis period. $[16^{th}, 84^{th}]$ confidence intervals are calculated using $10,000$ bootstrap replications as in Appendix A.

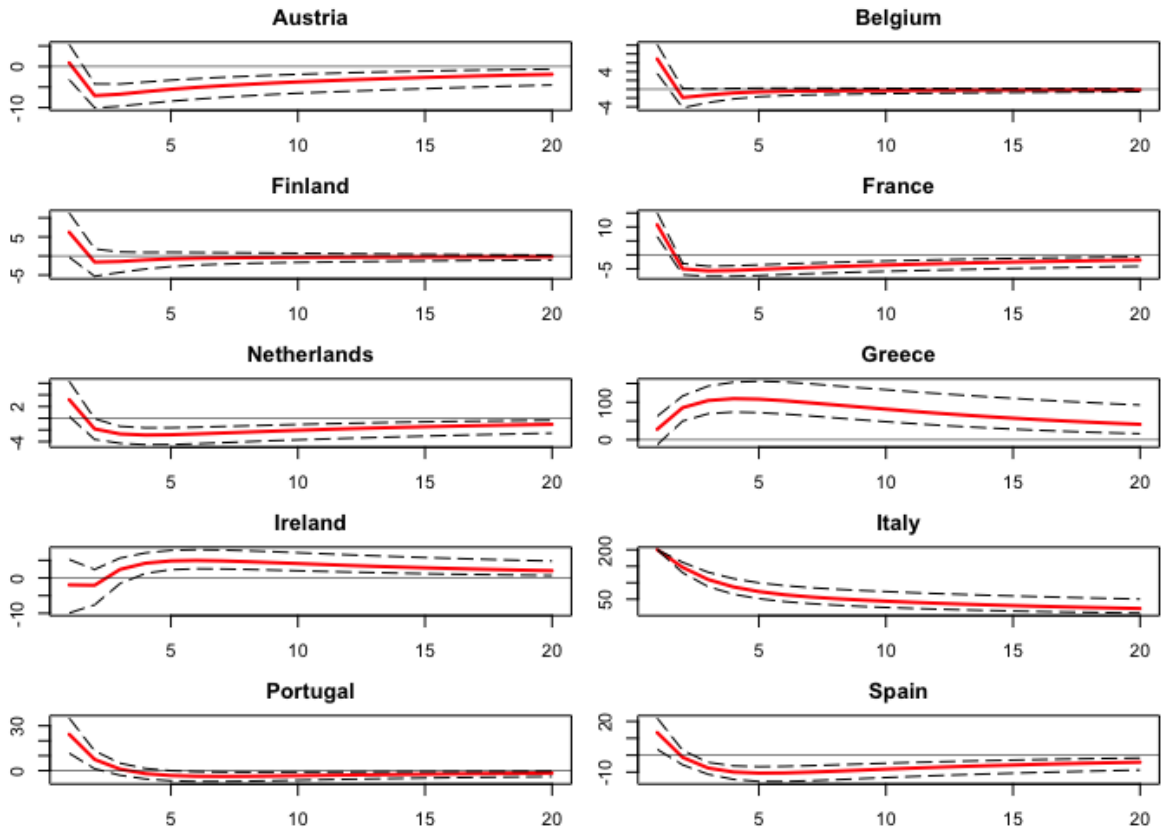

Figure A.14: The figure reports the Generalized Impulse Response Functions to a 200 b.p. shock to the $10Y$ Italian Spread in the COVID pandemic period. $[16^{th}, 84^{th}]$ confidence intervals are calculated using $10,000$ bootstrap replications as in Appendix A.

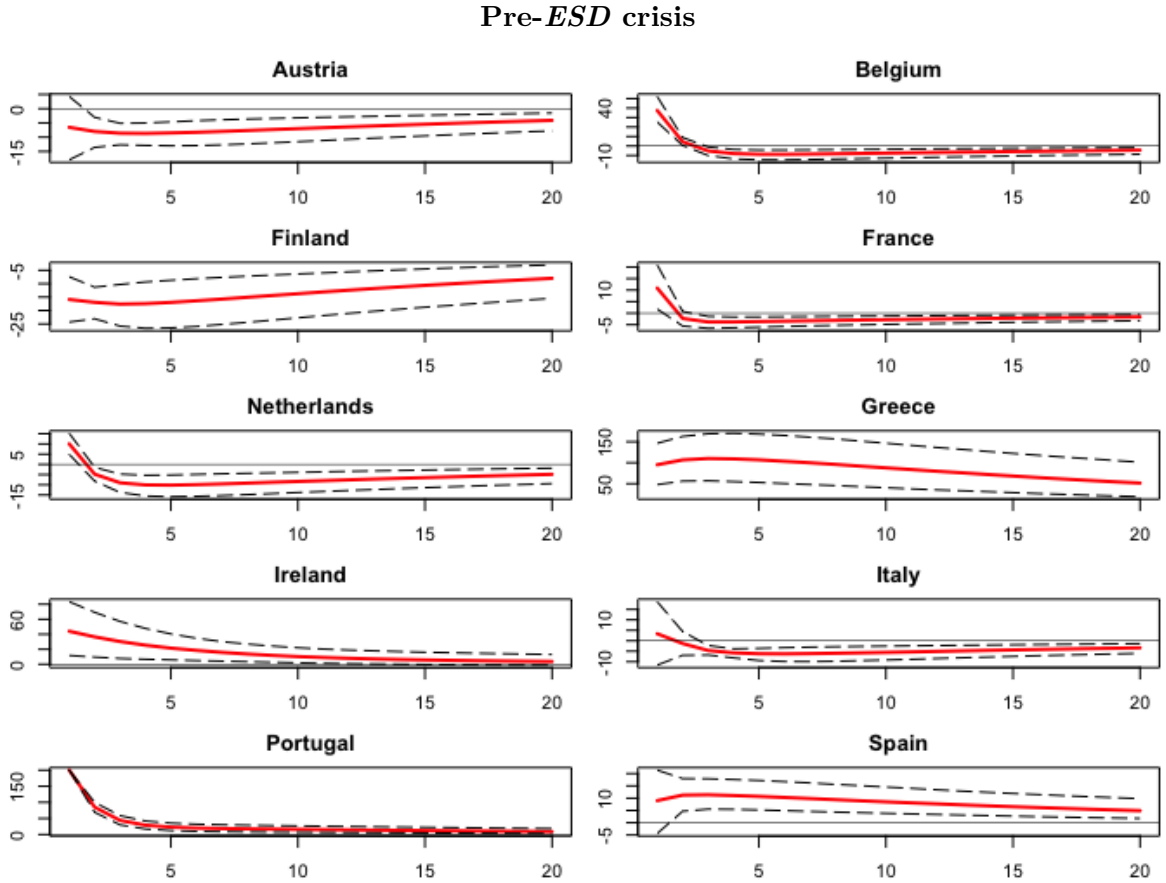

Figure A.15: The figure reports the Generalized Impulse Response Functions to a 200 b.p. shock to the $10Y$ Portuguese Spread in the pre-crisis period. $[16^{th}, 84^{th}]$ confidence intervals are calculated using $10,000$ bootstrap replications as in Appendix A.

Post-*ESD* crisis

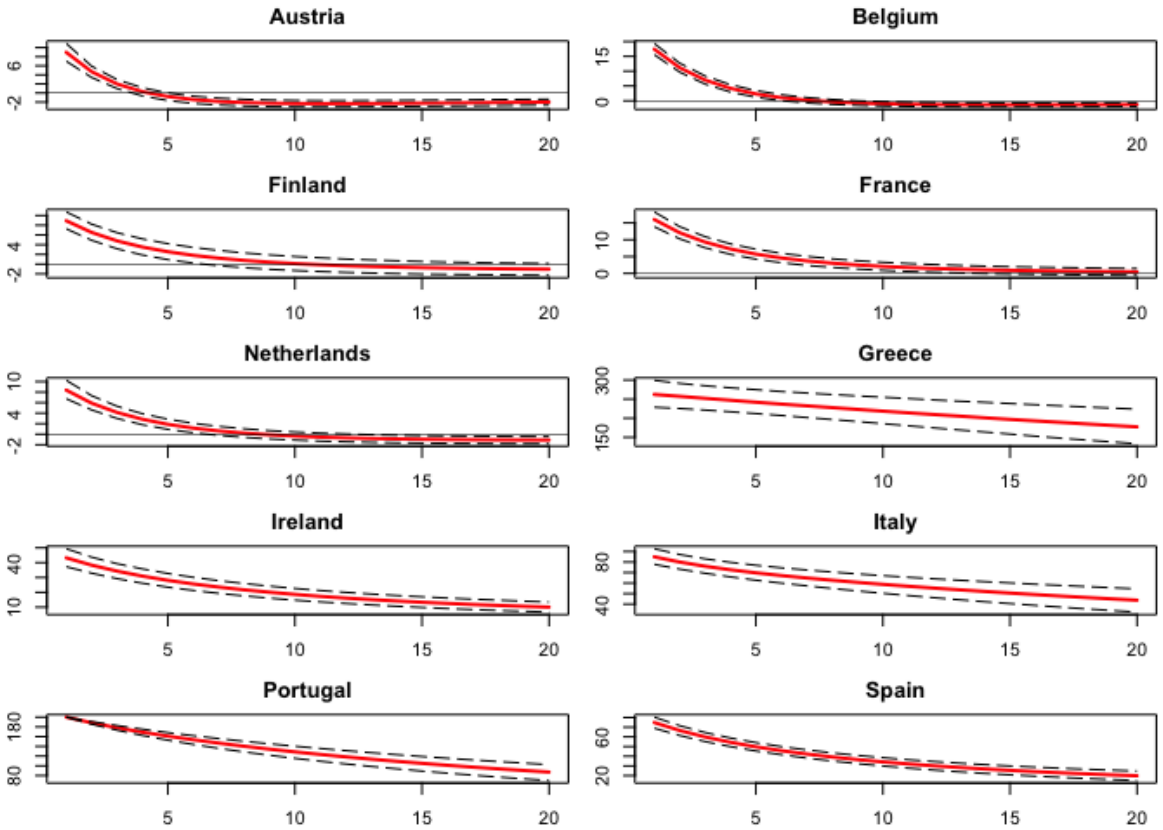

Figure A.16: The figure reports the Generalized Impulse Response Functions to a 200 b.p. shock to the $10Y$ Portuguese Spread in the post-crisis period. $[16^{th}, 84^{th}]$ confidence intervals are calculated using $10,000$ bootstrap replications as in Appendix A.

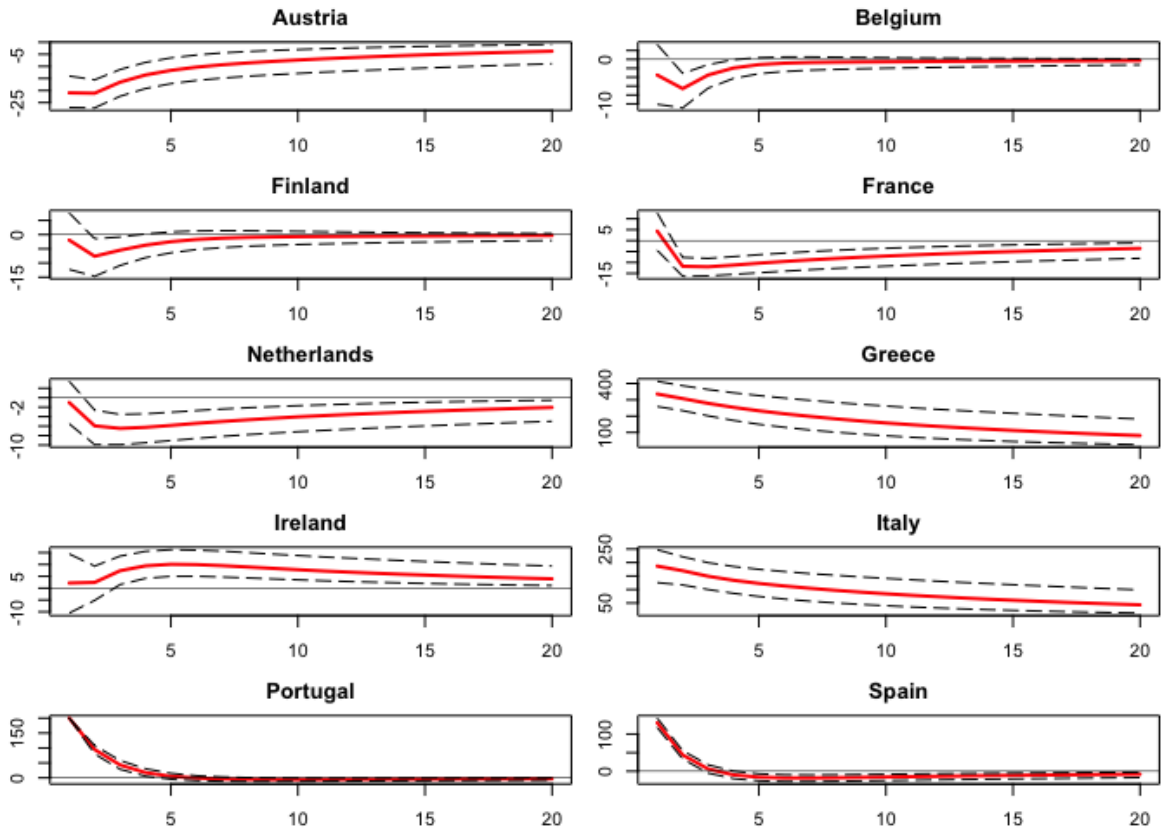

Figure A.17: The figure reports the Generalized Impulse Response Functions to a 200 b.p. shock to the $10Y$ Portuguese Spread in the COVID pandemic period. $[16^{th}, 84^{th}]$ confidence intervals are calculated using $10,000$ bootstrap replications as in Appendix A.